ν GC
the NUmerical Galaxy Catalog

矢作 日出樹
(東京大学天文学教室)
長島 雅裕
(長崎大学教育学部)
榎 基宏
(国立天文台天文データセンター)
郷田 直輝
(国立天文台ジャスミン検討室)
吉井 譲
(東京大学天文学教育研究センター)

ν GC = N-body + SA

- Dark matter carries most of mass in the Universe
  - Galaxies are baryonic components accumulated at the bottom of the potential well generated by dark matter
  - We can treat the evolution of dark matter distribution (by N-body method) and evolution of galaxies (by Semi-analytic model; SA) separately
- Spatial distribution →N-body
- Other observable quantities →SA
- Kauffmann et al. (1999)

Parameters of *N*-body simulation

- Computer: VPP-5000 (@ ADAC/NAOJ)
- Number of particles: 512^3
- Cosmological parameters:

$$\Omega=0.3,\ \lambda=0.7,\ \sigma_8=1.0$$

- Box size: $70h^{-1}$ Mpc

Cluster Finding Algorithm

- Friends-of-Friends method
  - A pair of particles separated within the linking length belongs to the same group
  - Percolation of spheres whose radius is the linking length

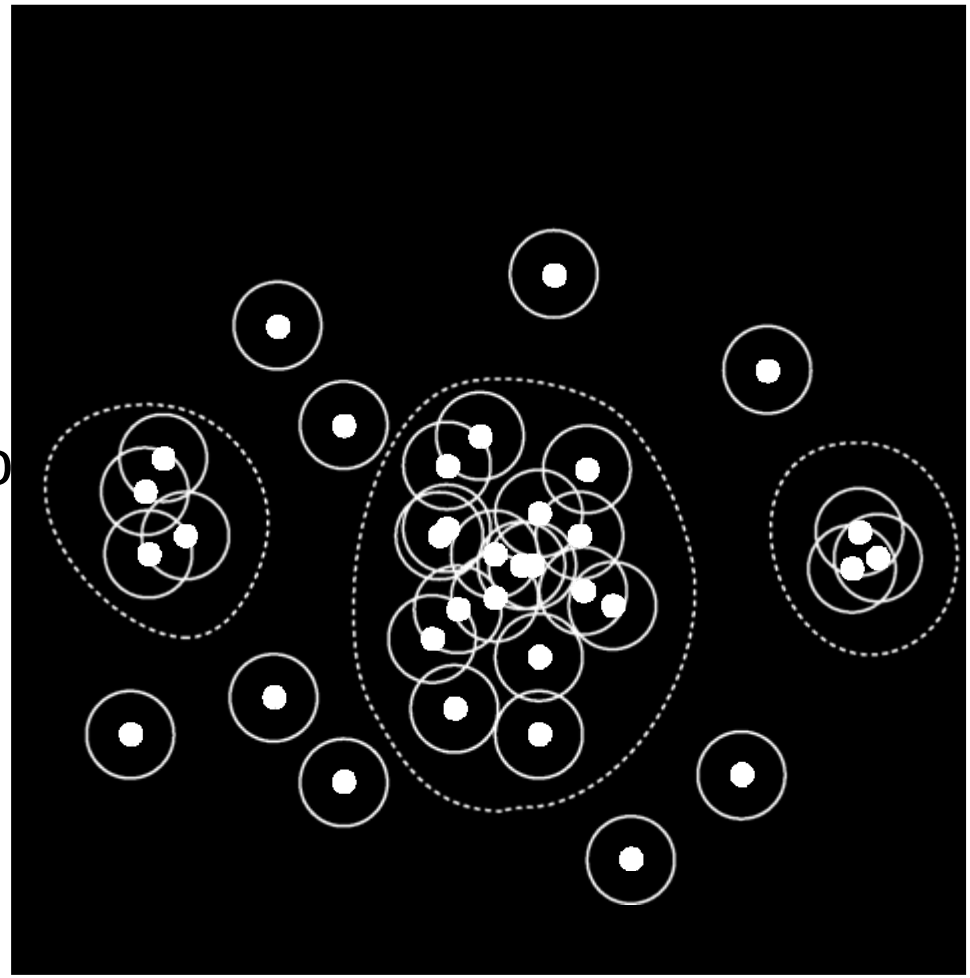

Mass Function of Dark Halos

- Effective mass resolution is several $10^{10}M_{\odot}$
  (L = $70h^{-1}$Mpc)
- Well-fitted by Sheth-Tormen type mass function

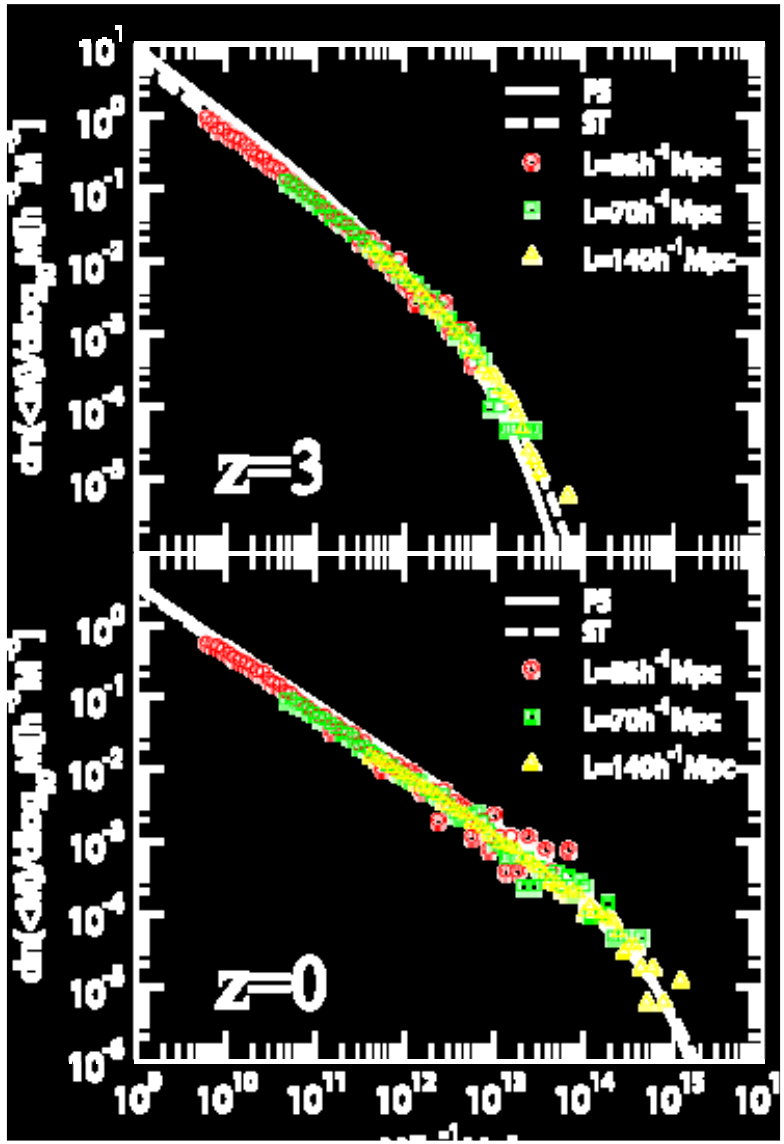

Merger Trees of Dark Halos

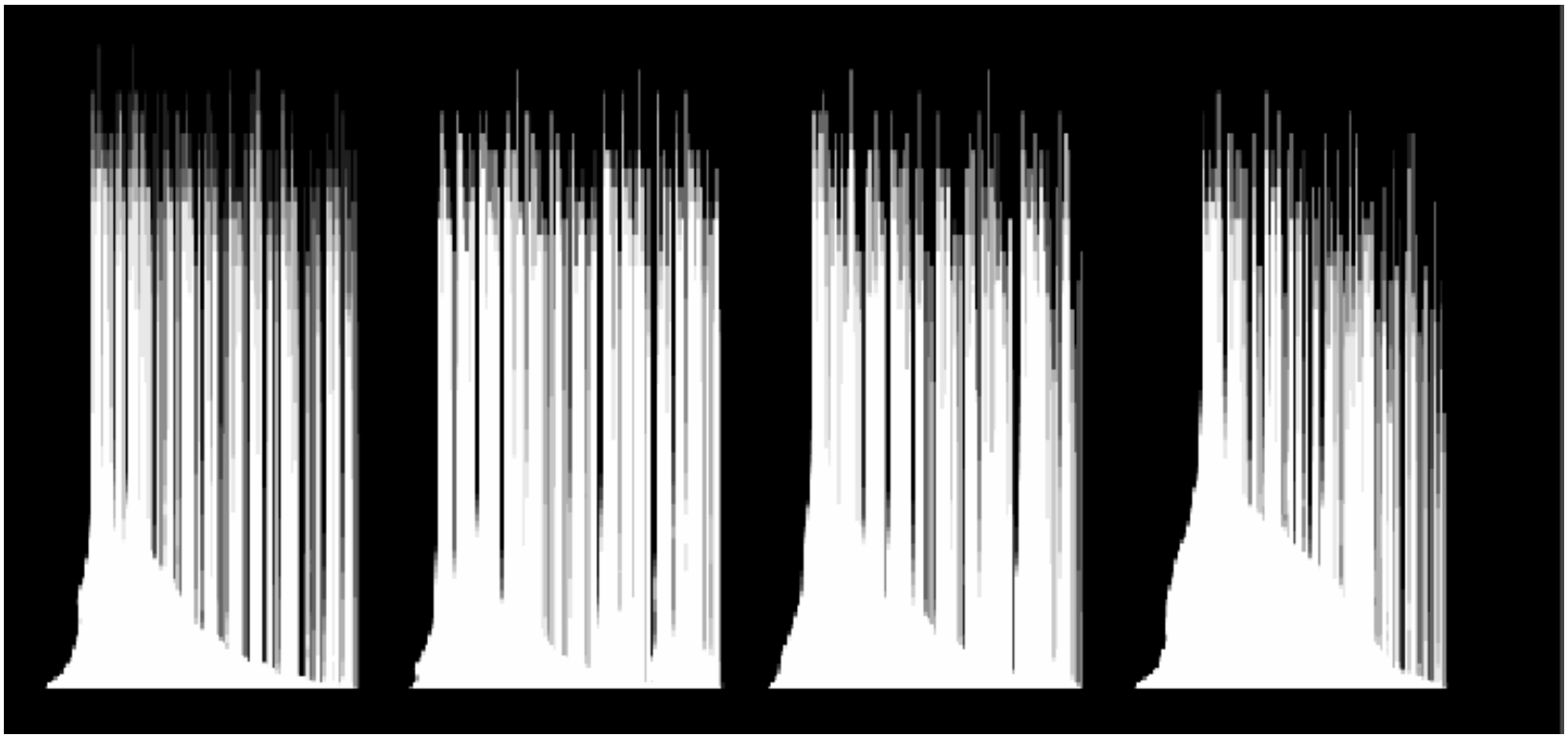

ν GC

- ループがあった場合、強制的にくっつけて一つのハローと看做す

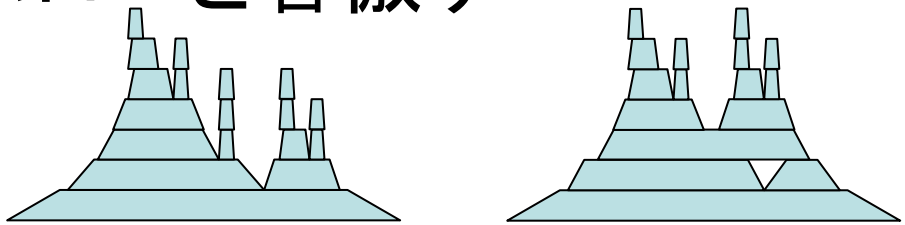

ループの無いツリー　　ループの有るツリー

  - ループができる原因
    - オフセット衝突で侵入ハローが標的ハローの外側を掠める
  - では、マージャーツリー中にループはどのくらいあるのか?
    - 218856(ループ消去前)→ 114428(後)

ループ統計

- ループ消去で消されたハローの質量関数

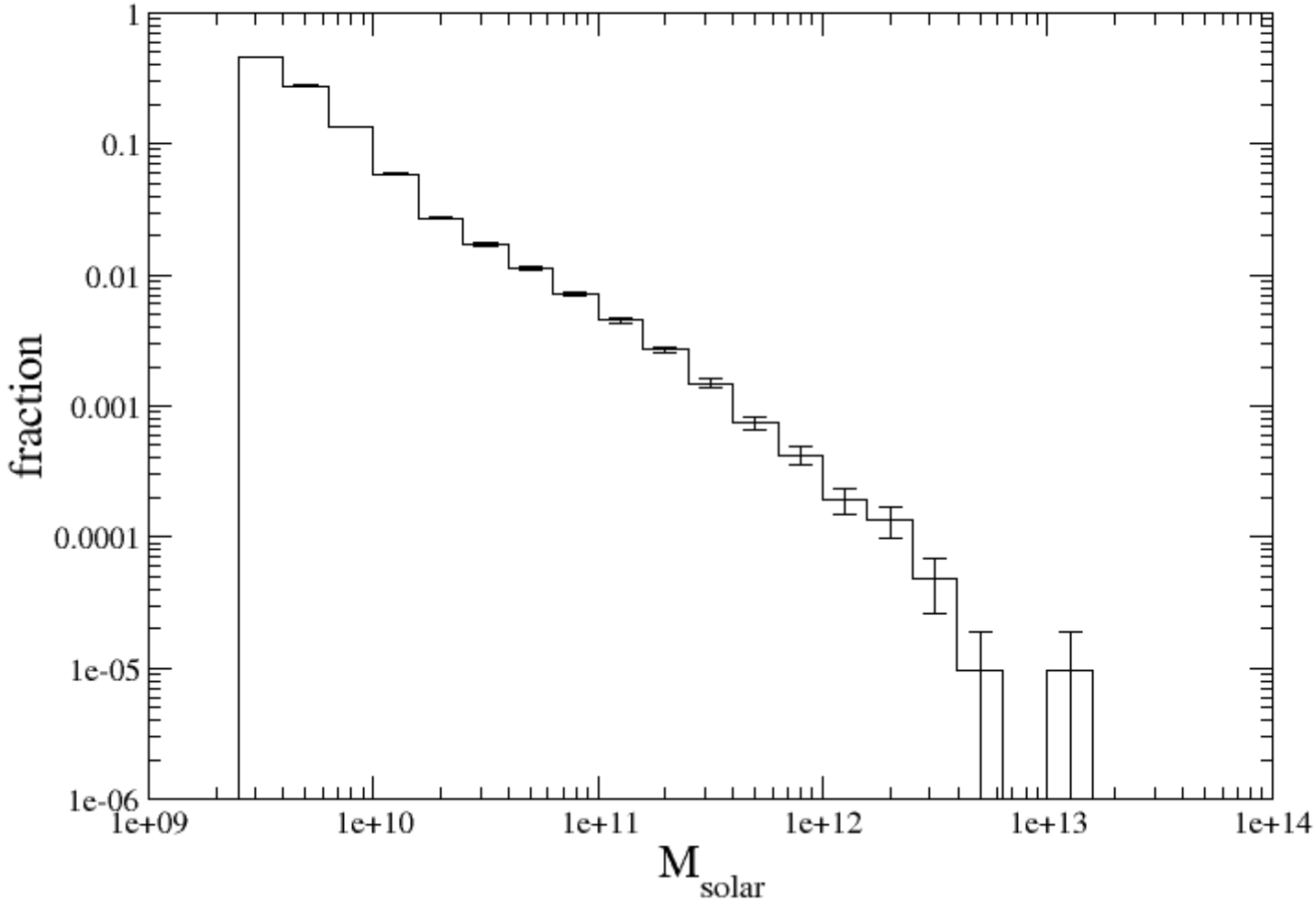

ループ統計

- 9割近くは$10^{10}M_{\odot}$以下の小さなハロー

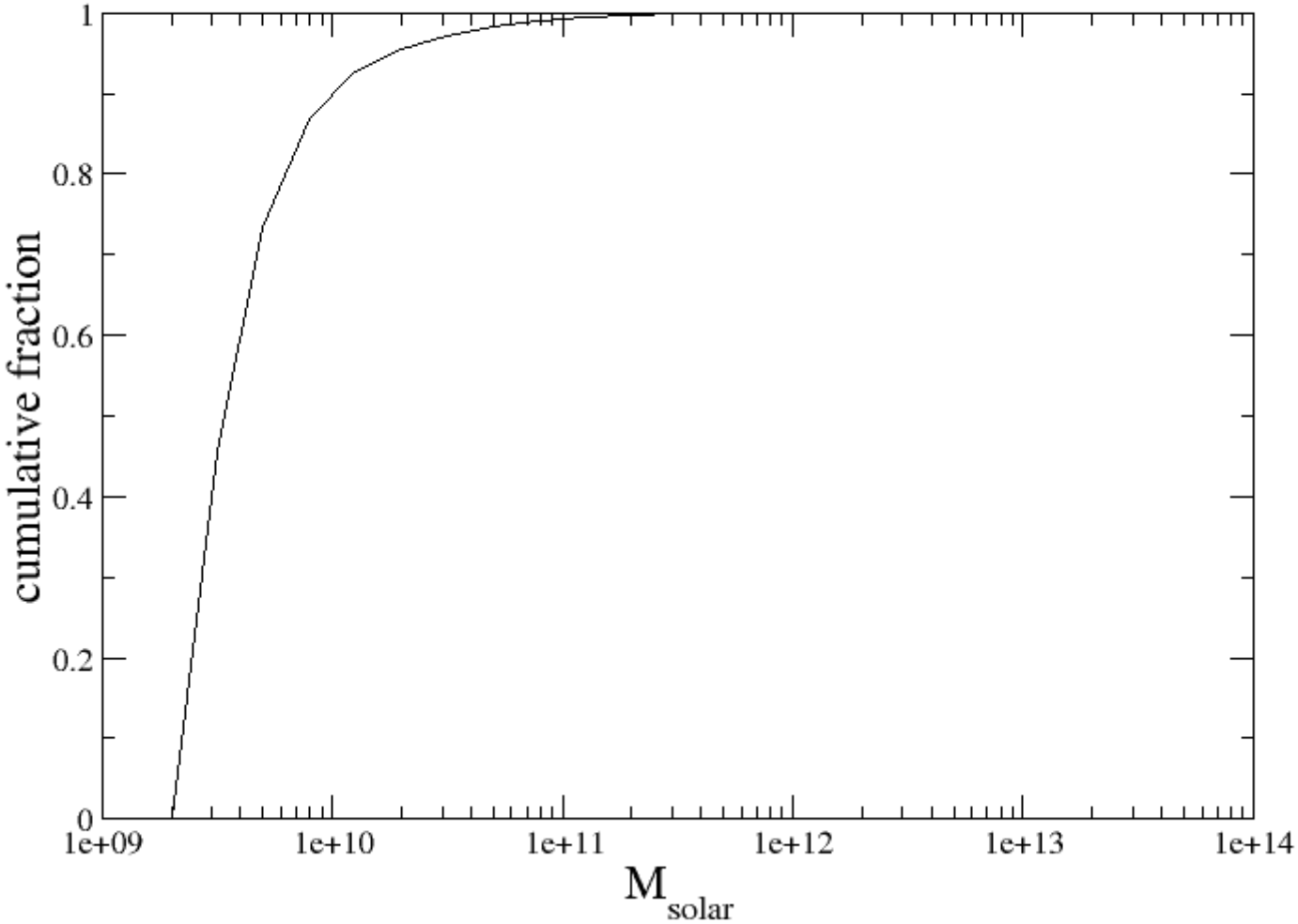

ループ統計

- ループハローの質量とツリーハローの質量比分布

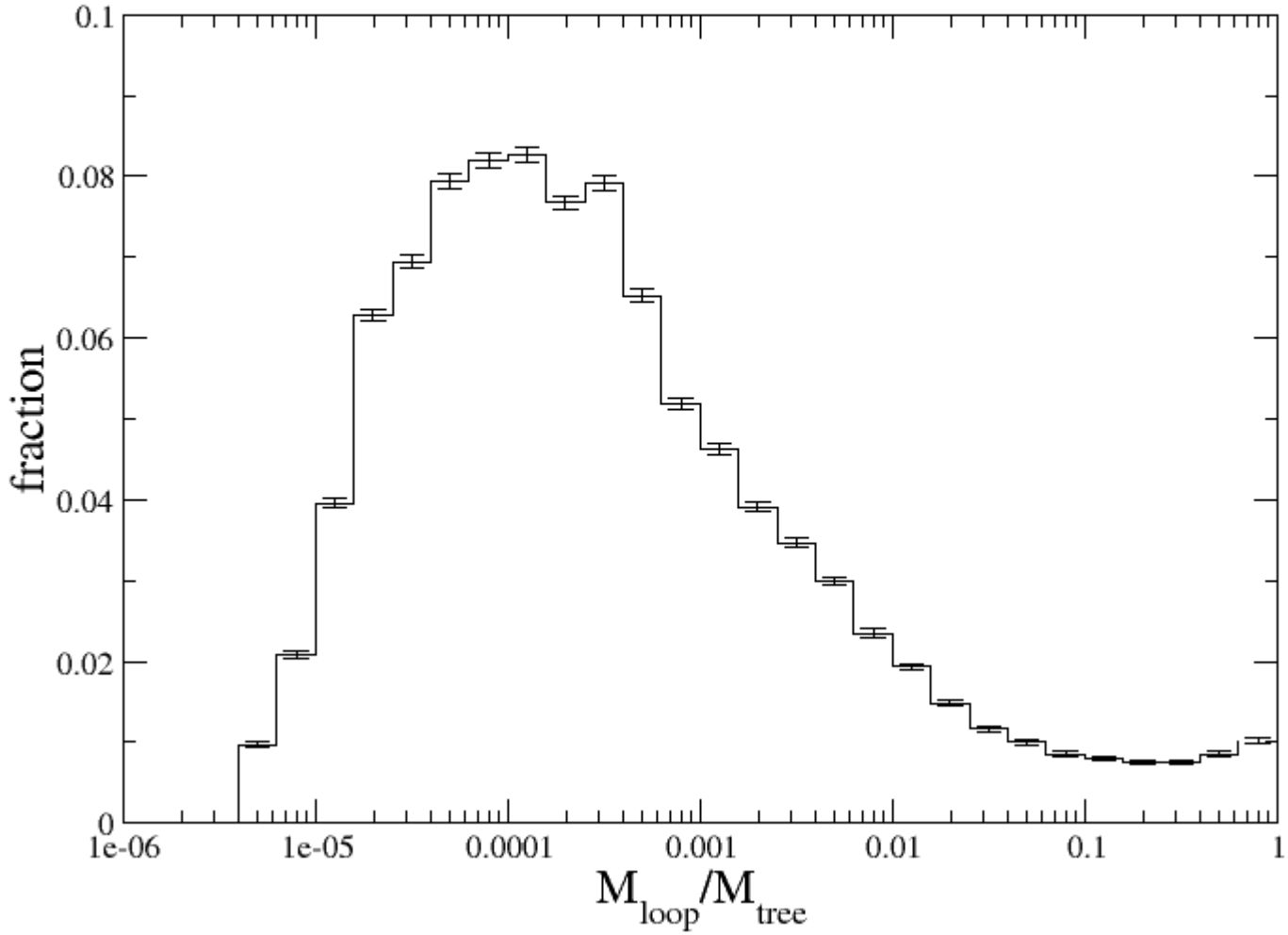

ループ統計

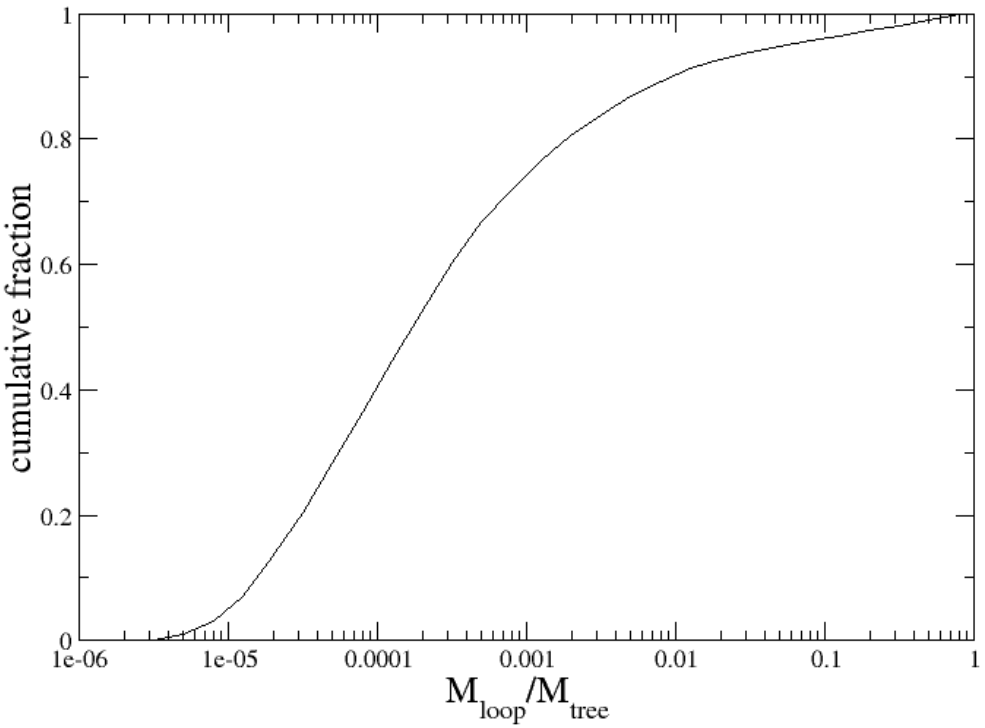

- Major Merger
  - (M_{loop}/M_{tree}>0.5)
  - ~1.6%
- Minor Merger
  - (M_{loop}/M_{tree}<0.1)
  - ~96%

まとめ

- ループハローは全体の約半数を占める
  - 更にその9割以上は$10^{10}M_{\odot}$(N<30)以下の小さなハローが占めている
- ループハローとツリーハローの比の分布を調べた
  - 10^{-4}近辺にピークを持つ分布
  - 殆どが Minor Merger によってできたループである

Semi-Analytic Model

- Nagashima et al. (2001)

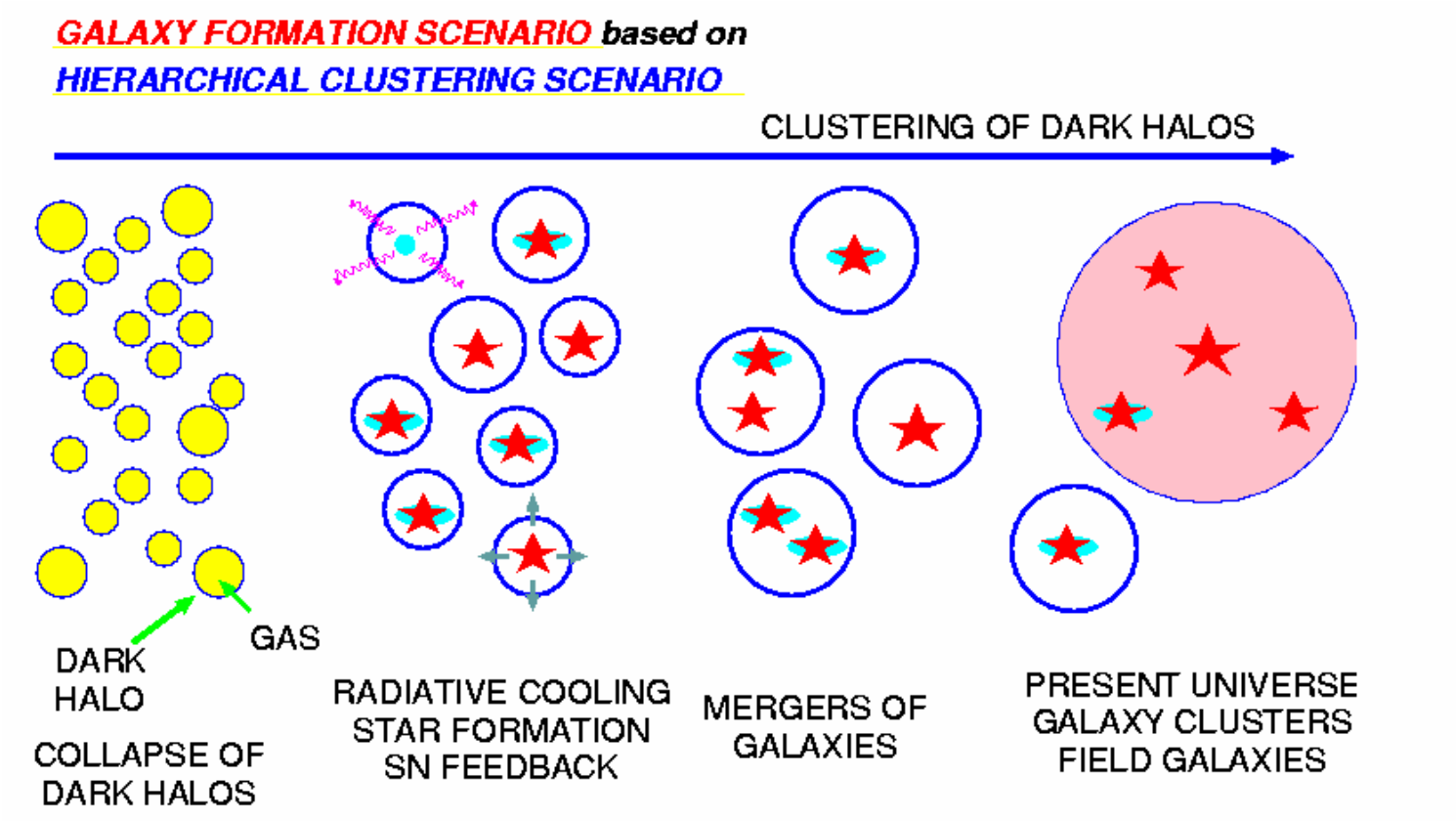

Semi-Analytic Model

Mergers of Galaxies

When dark halos merge:

- Hot gas components merge immediately
- Dividing galaxies into CENTRAL and SATELLITES

CENTRAL: central galaxy in the most massive progenitor

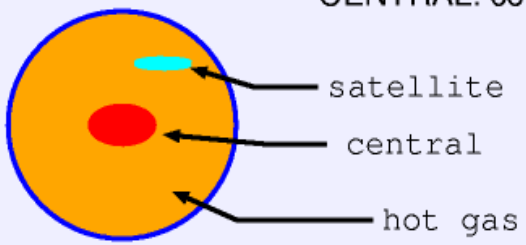

Criteria of galaxy mergers:

$t_{elapse} > t_{fric}$ (dynamical friction time-scale) satellite-central merger

$\Delta t > t_{coll}$ (random collision) satellite-satellite merger

Types of mergers:

Merger of similar mass galaxies: STARBURST + BULGE FORMATION (MAJOR MERGER)

Otherwise: Smaller galaxy is incorporated into disk of larger galaxy (MINOR MERGER)

Semi-Analytic Model

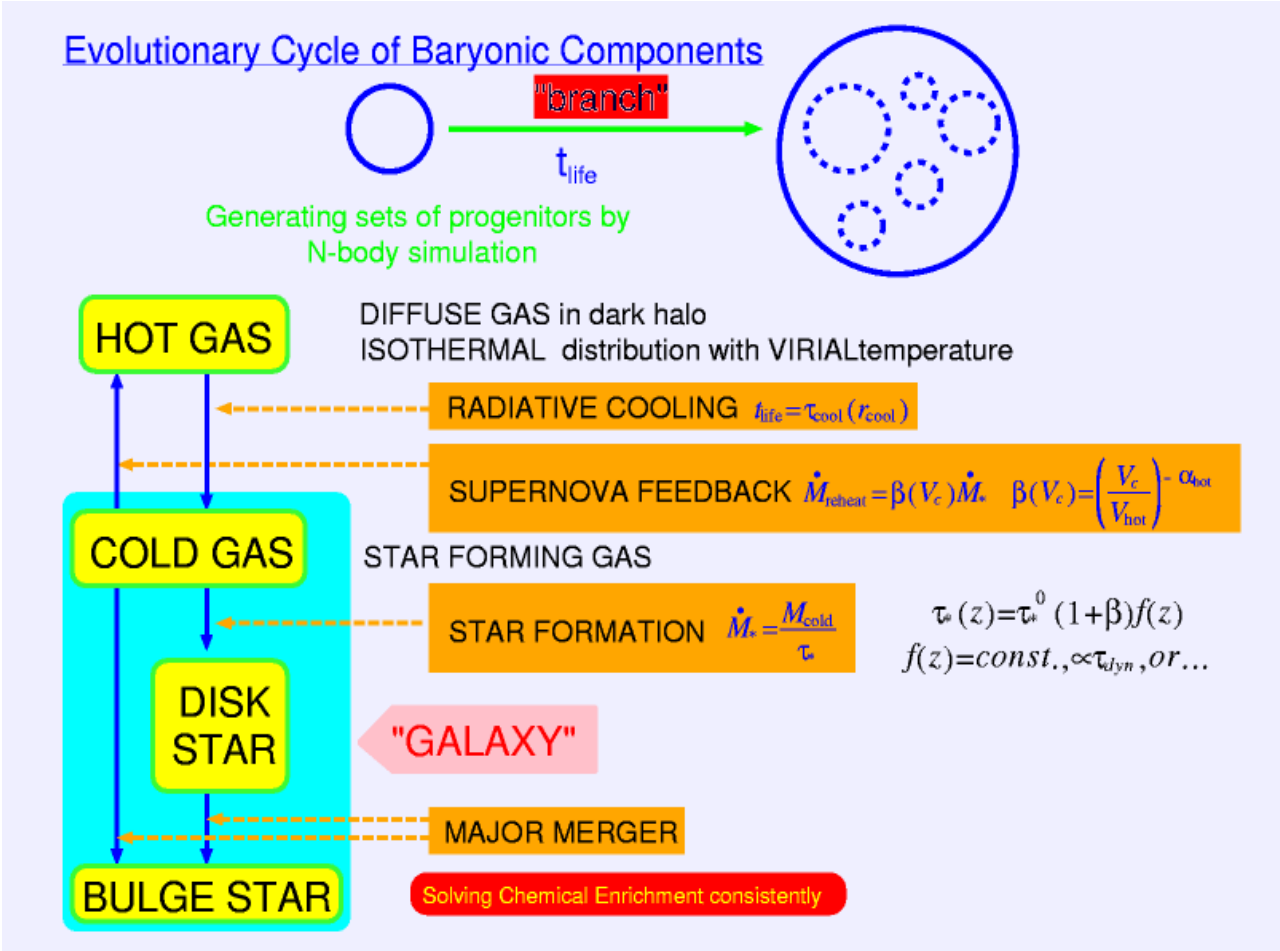

Semi-Analytic Model

3. Parameter normalization

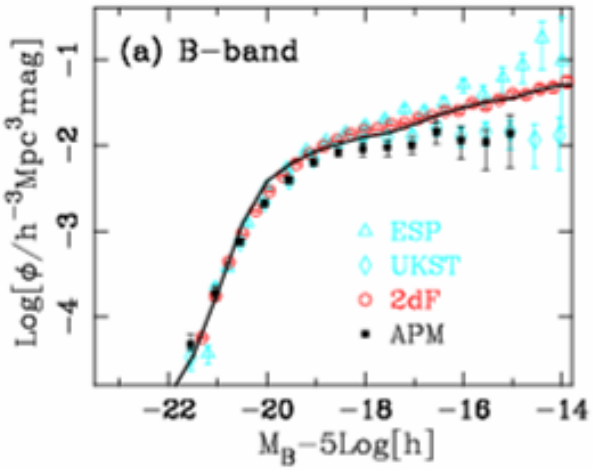

Luminosity Functions
(SN feedback parameters)

Cold gas mass fraction
(SF time-scale)

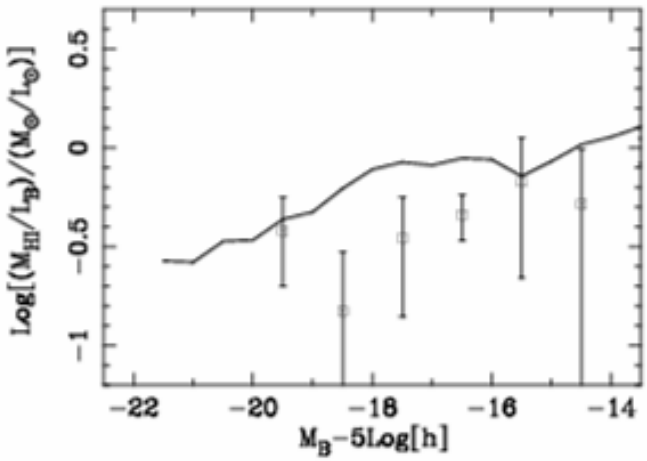

Semi-Analytic Model

Disk size

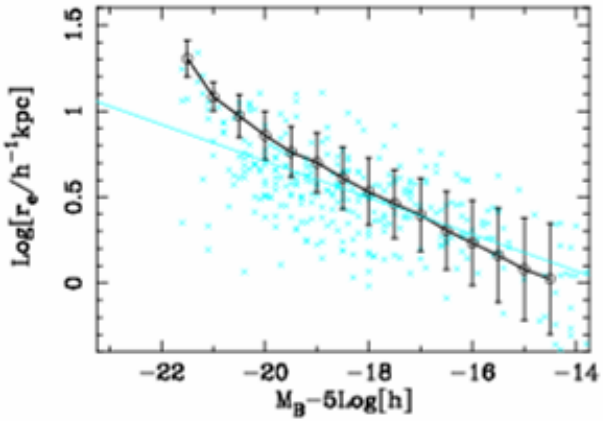

Galaxy Counts

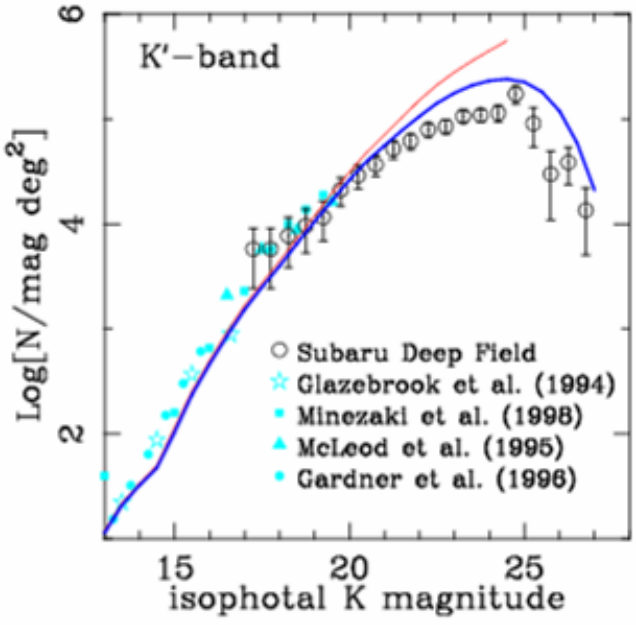

Parameter set:

$\Omega_0 = 0.3, \Omega_\Lambda = 0.7, \sigma_8 = 1, h = 0.7$

$V_{hot} = 120 km/s$

$\alpha_{hot} = 4$ SN feedback

$\tau_*^0 = 1.7 Gyr$ SF time-scale

$f_{merge} = 1.8$ Merger time-scale

$f_{bulge} = 0.5$ Major merger criterion

(preliminary results)

Distribution of Dark Matter and Galaxies

- z=0

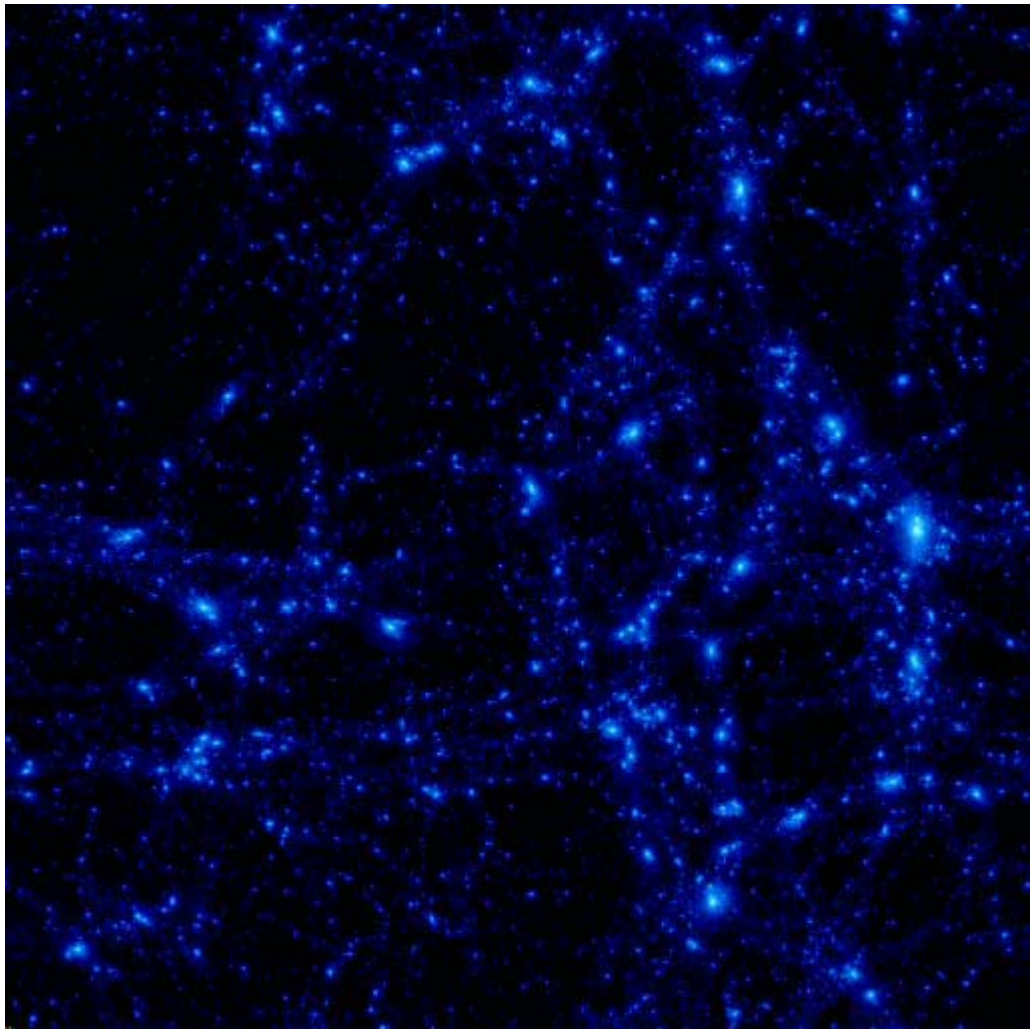

Distribution and Colors of Galaxies in the Cluster

- Cluster at z=0

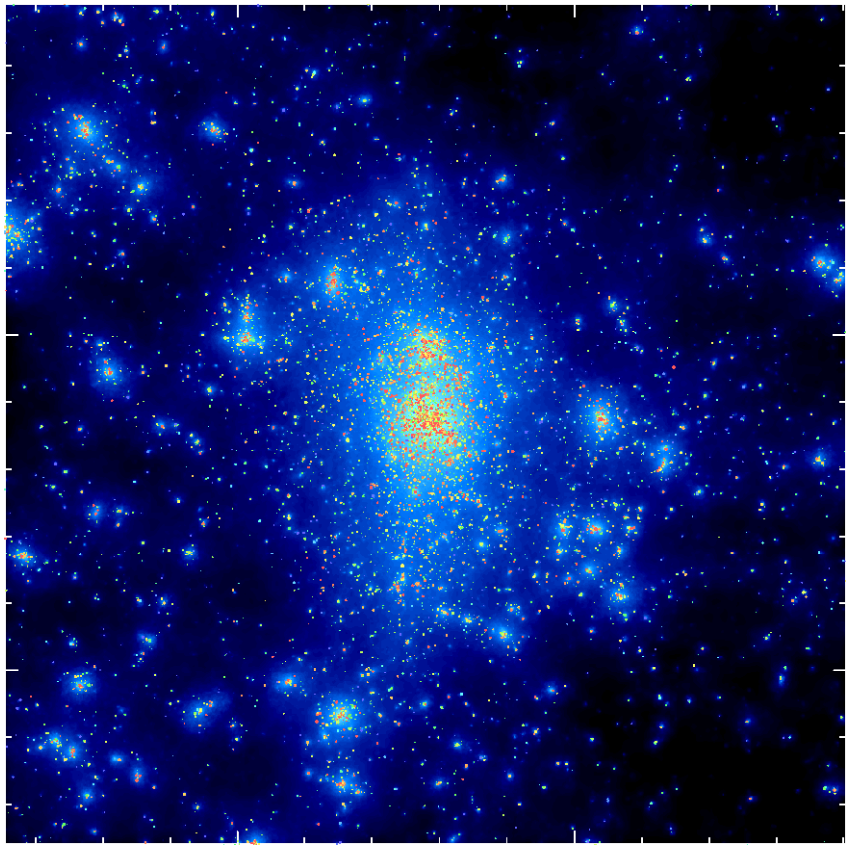

Distribution and Colors of Galaxies in the Cluster

- Cluster @z=0.5

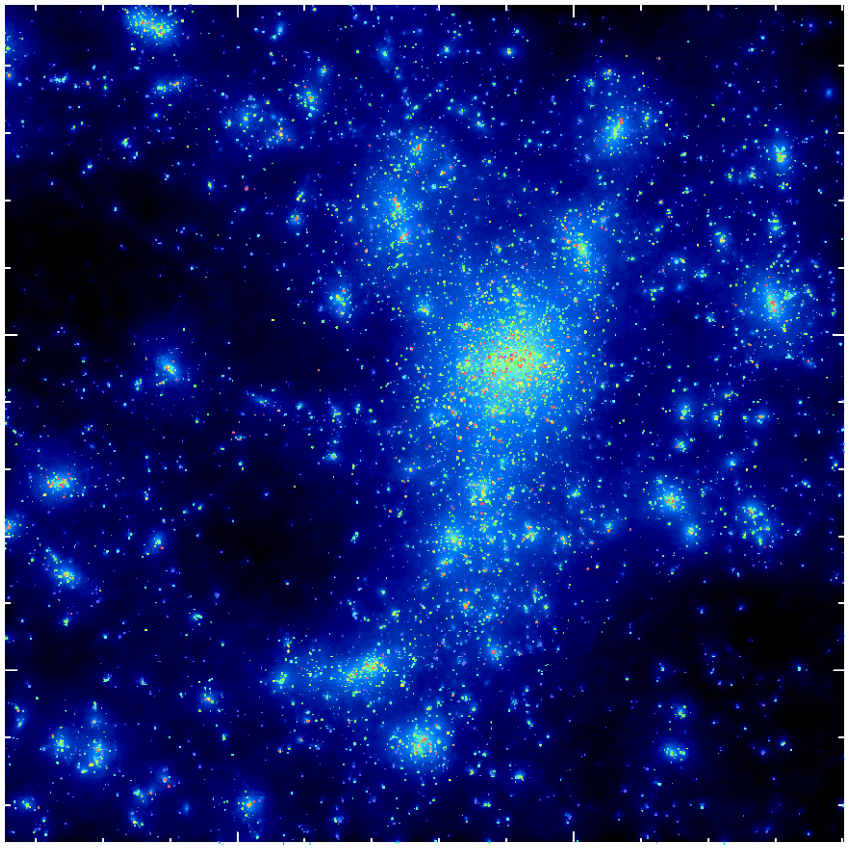

Distribution and Colors of Galaxies in the Cluster

- Cluster at z=1

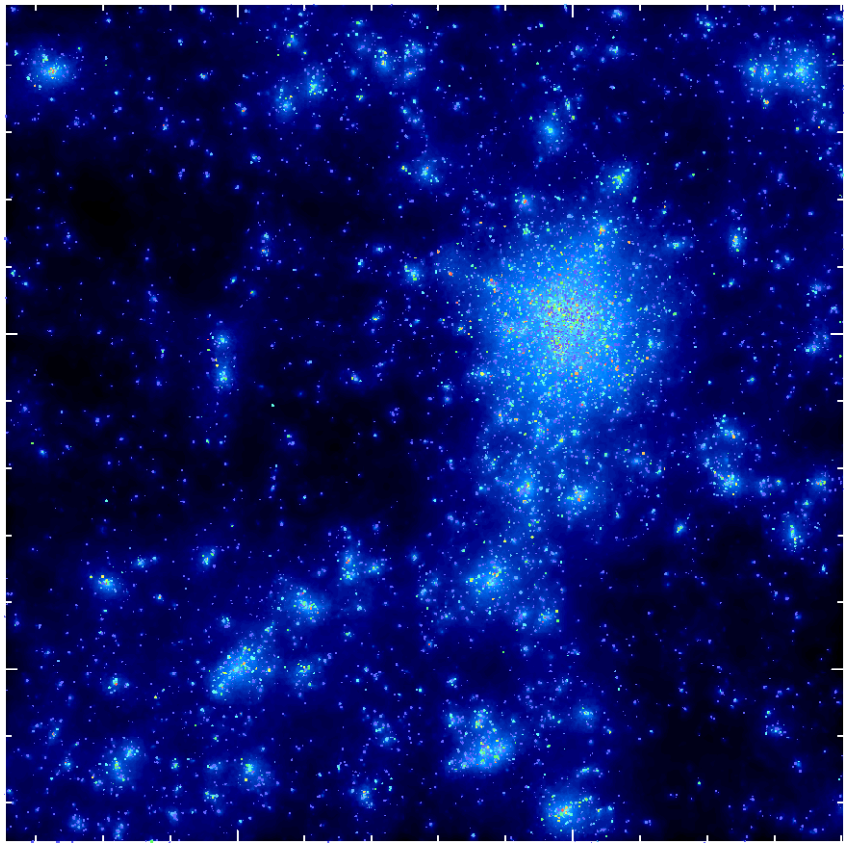

Applications of ν GC

- Angular correlation function of galaxies
  - Yahagi, Nagashima, Miyazaki, Gouda, & Yoshii
- Extragalactic background fluctuation
  - Nagashima, Yahagi, & Yoshii
- Cosmic string search
  - Japanese Virtual Observatory groups

Angular Correlation Function

- Wedge diagram

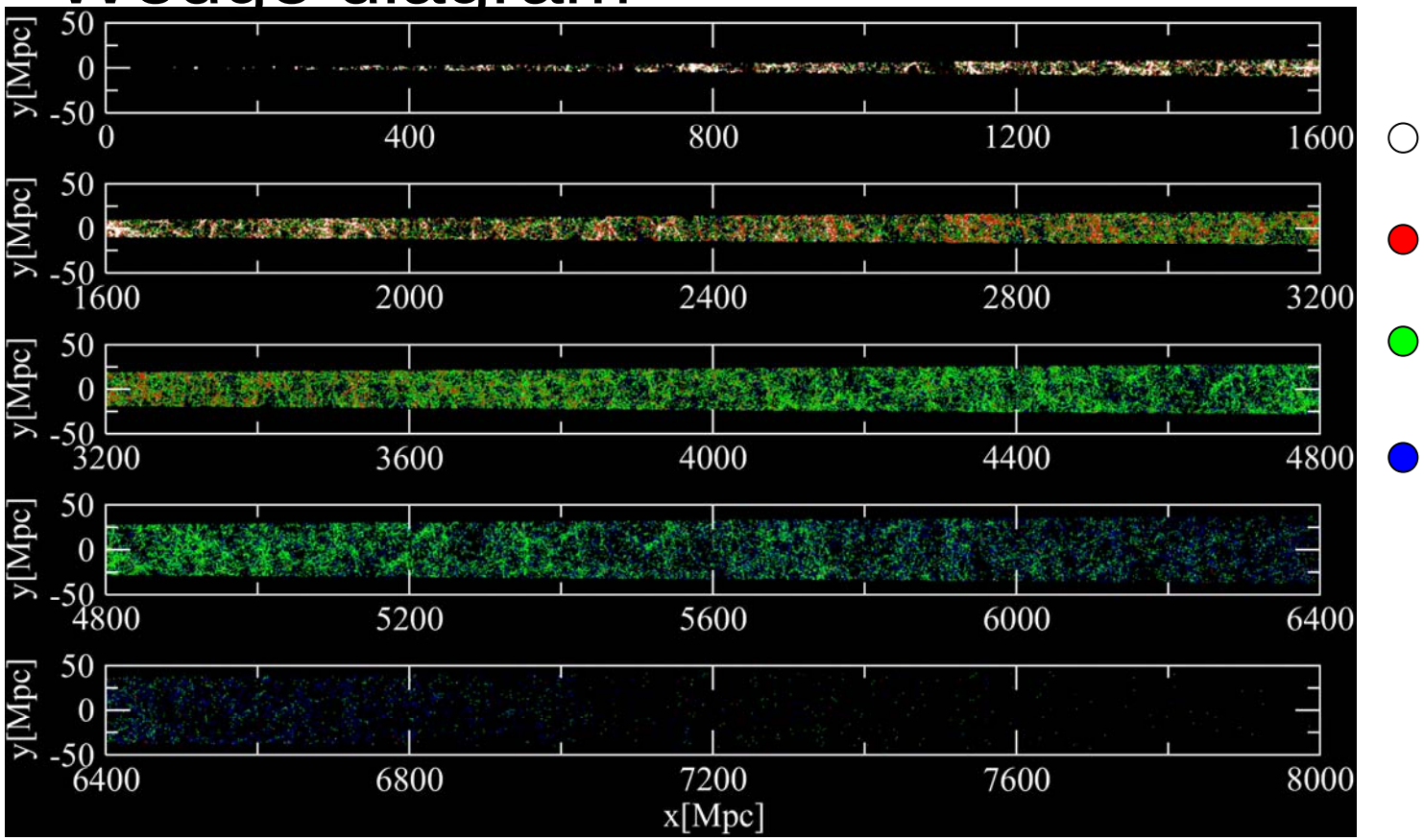

Angular Correlation Function

- Field-to-field variation

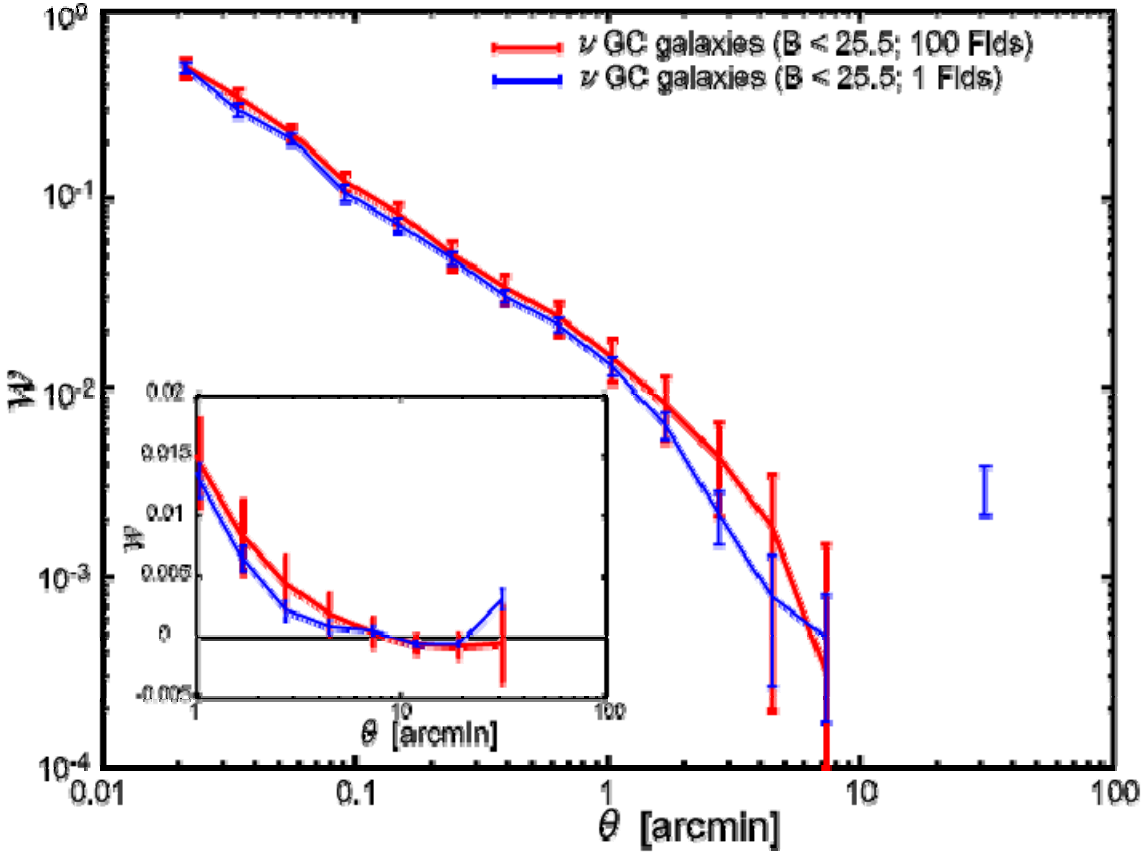

Angular Correlation Function

- Integral Constraints

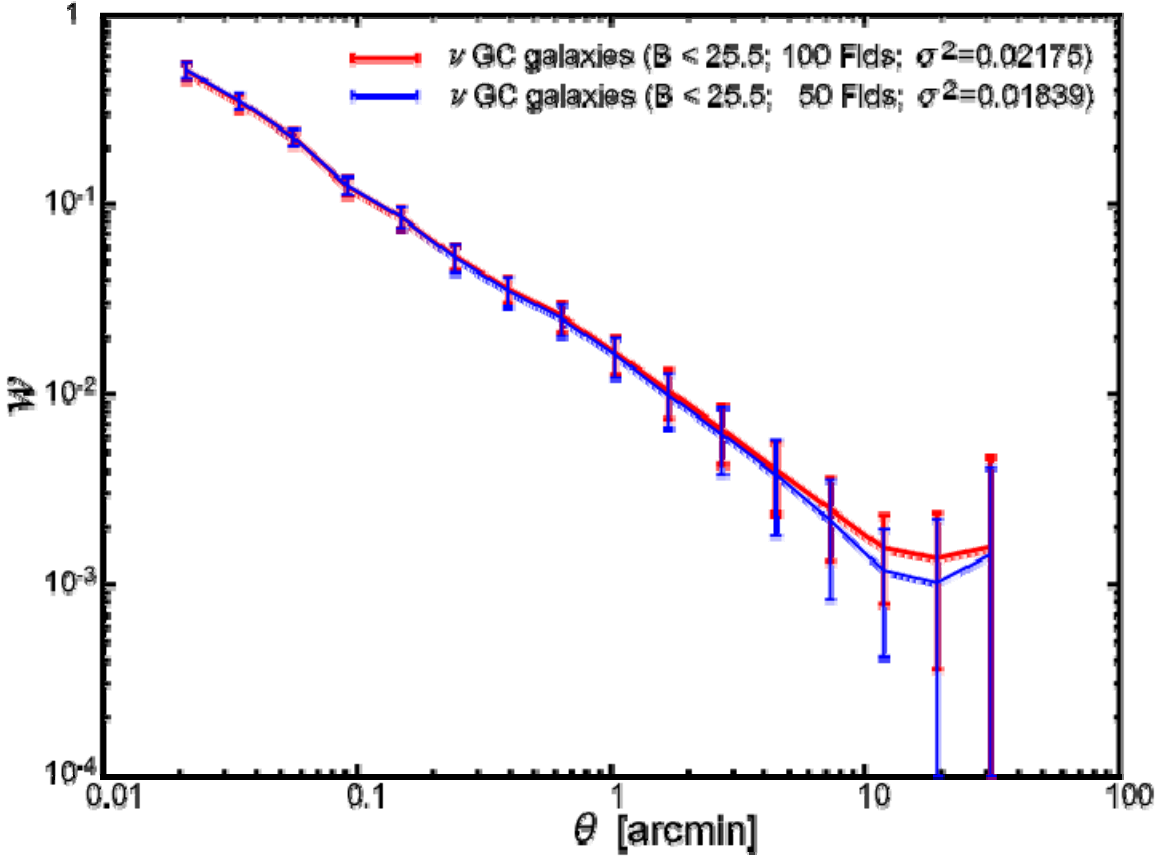

Angular Correlation Function

- Limiting magnitude

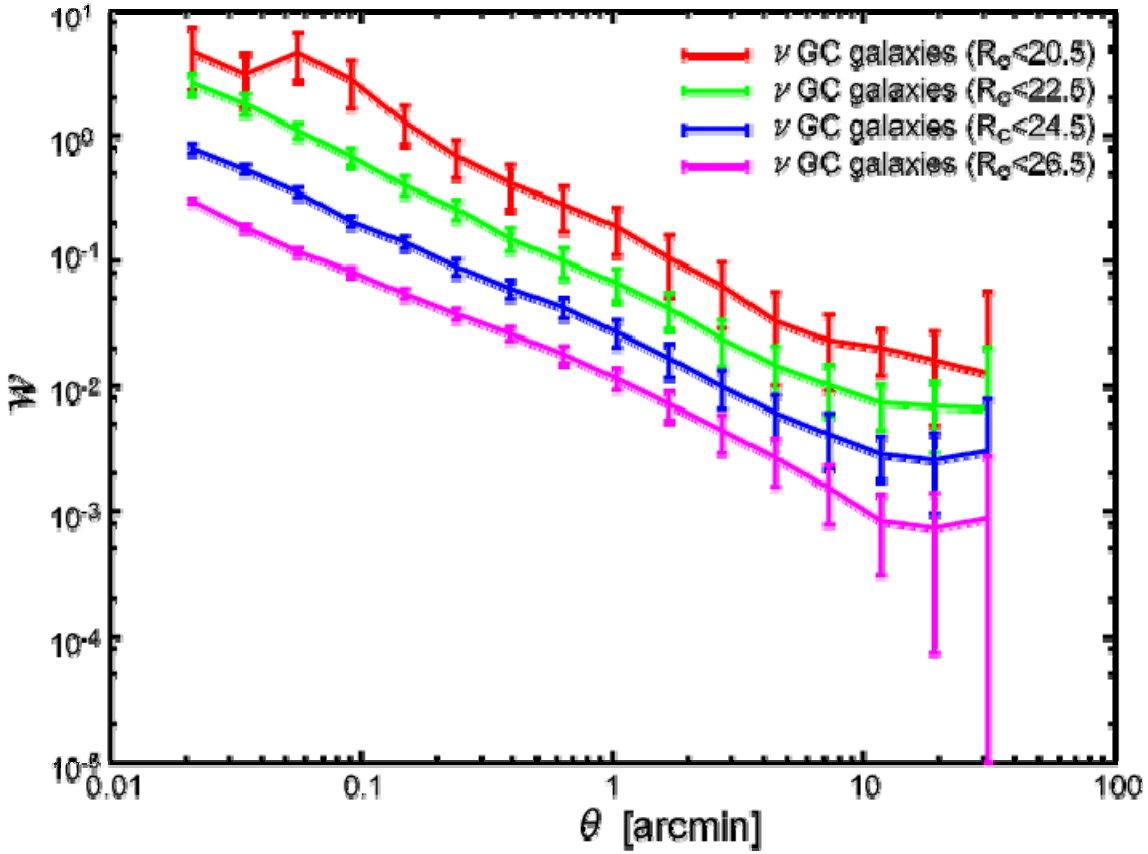

Angular Correlation Function

- Subaru Suprime-Cam
  - GTO 2.2 deg^2 field
    - S. Miyazaki (Subaru telescope, NAOJ) et al.

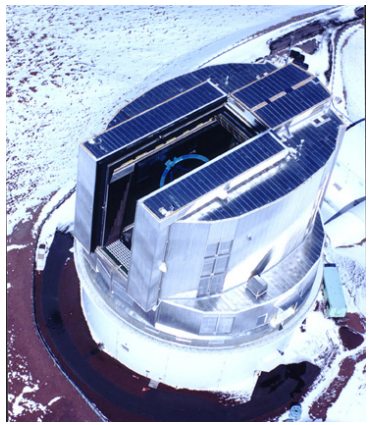

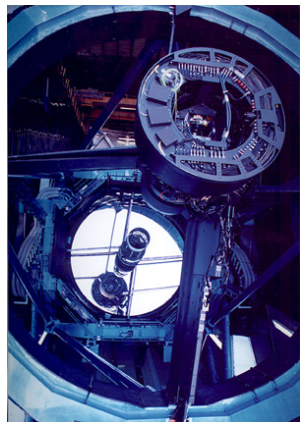

Angular Correlation Function

- Comparison with observational data

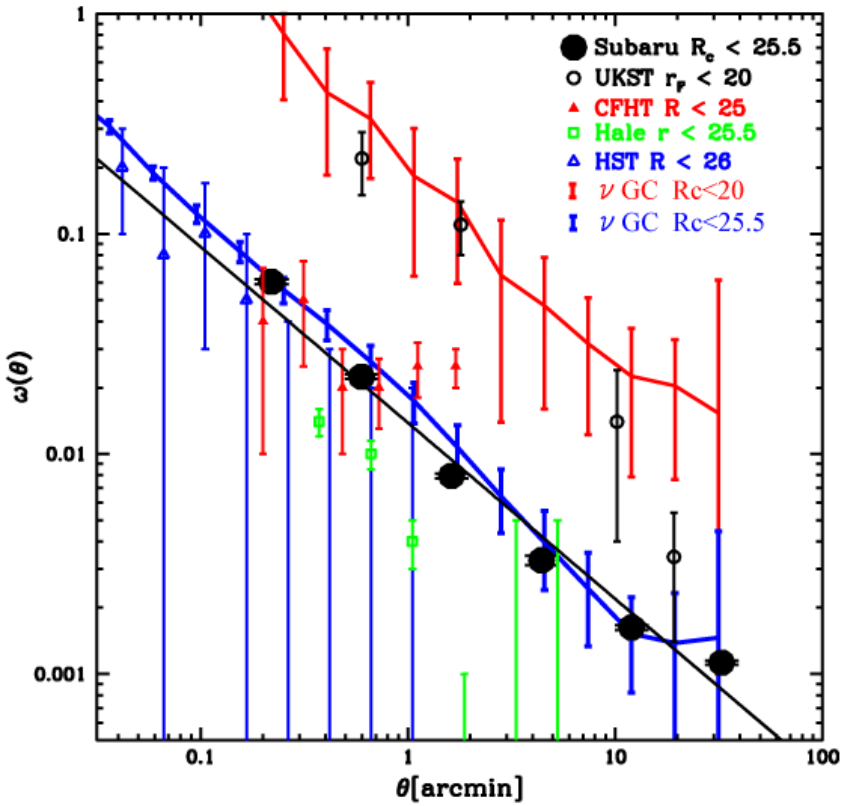

Cosmic Background Radiation

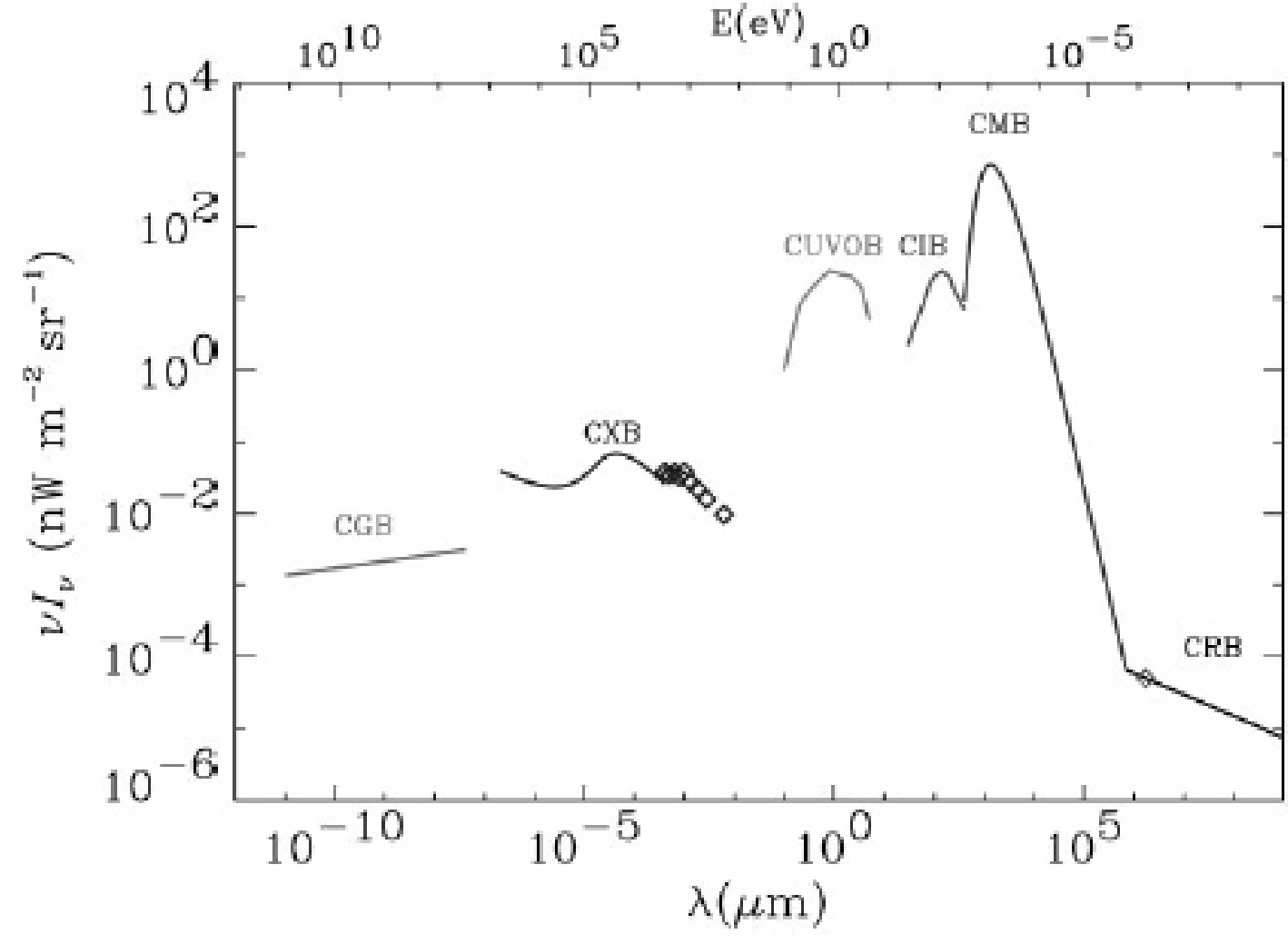

Cosmic Microwave Background

- WMAP

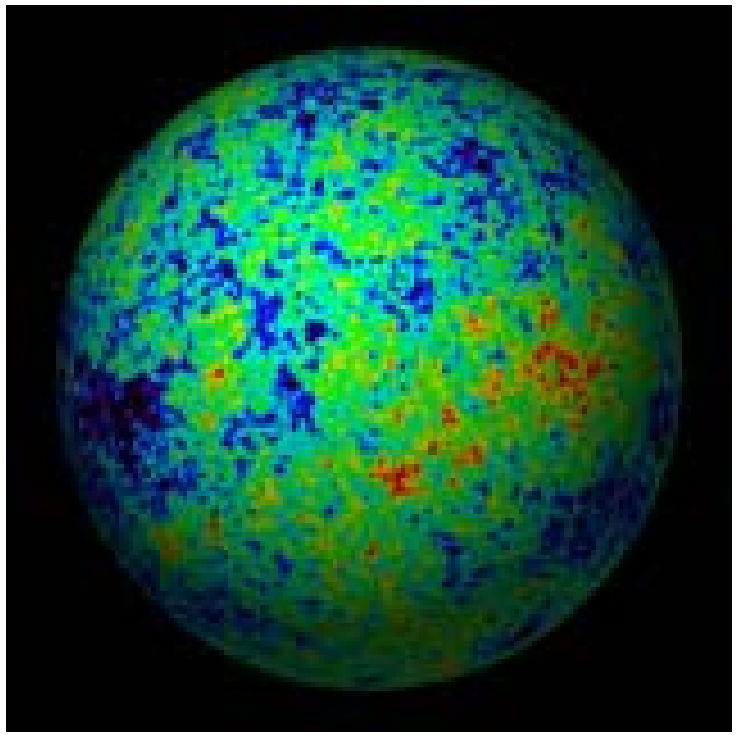

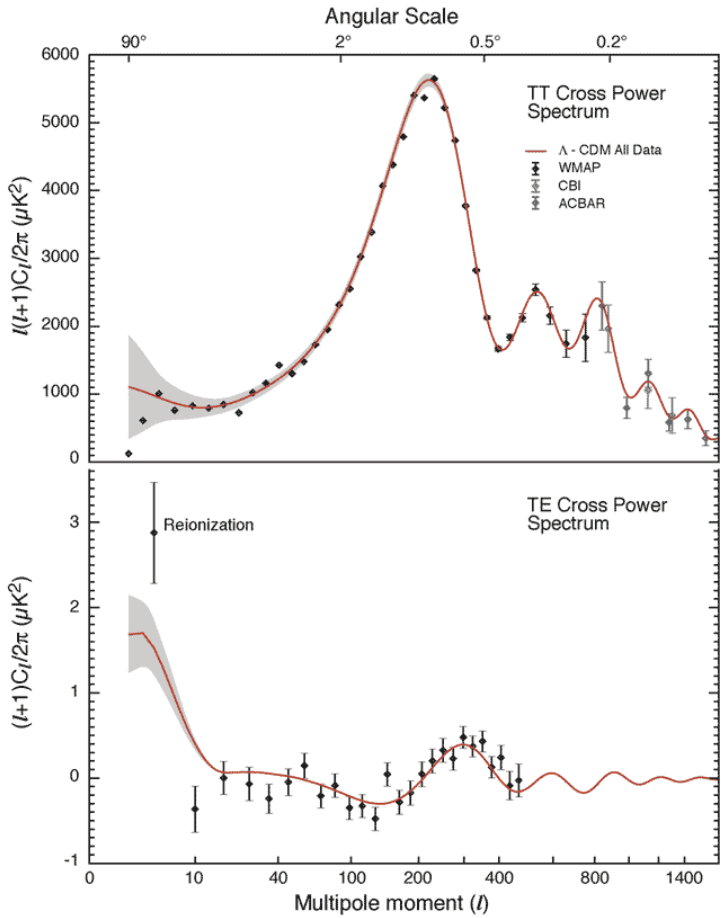

Cosmic far-IR Background

- ISO

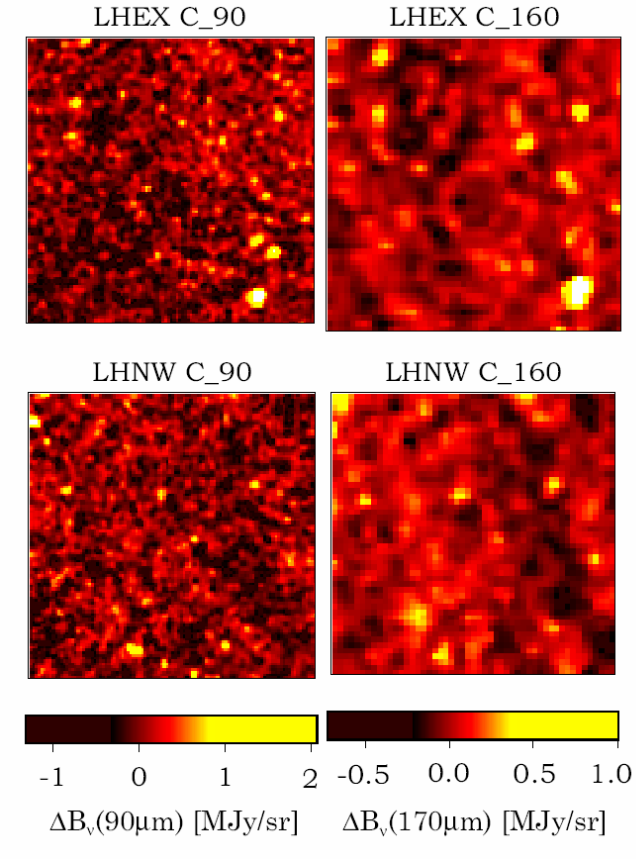

Fig. 1. The left column shows 90 μm images of LHEX (top) and LHNW (bottom). Each image is $39'.5 \times 39'.5$ wide ($23''$/pixel). The right column shows 170 μm images ($46''$/pixel). The LHEX image is $40'.6 \times 40'.6$ wide, while the LHNW one is $39'.1 \times 39'.1$ wide. The brightness shown in each image is offset from its median brightness. Each image is made of four $22' \times 22'$ sub-fields. Roughly the north is left and the west is top.

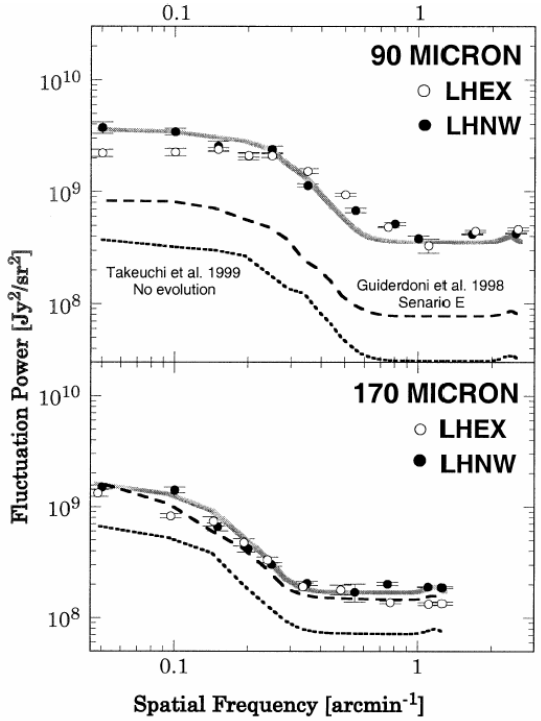

Fig. 3. The residual PSDs of 90 μm (top) and 170 μm (bottom) images (open circles and filled circles, same as Fig. 2) are compared with the simulated PSDs based on various number counts models: dashed lines are PSDs of the simulated images by Guiderdoni et al. (1998) scenario E, while the dotted lines are those by Takeuchi et al. (1999) no-evolution. Thick gray lines are examples of the simulated images produced by simple double power-law number count models (see text for details).

Cosmic near-IR Background

- ISO

TABLE 2 Measurements of infrared background fluctuations

λ (μm)	θ[a] (arcmin)	$\delta(\nu I_\nu)$[b] (nW m^{-2} sr^{-1})	P_S[c] (Jy^2 sr^{-1})	νI_ν[d] (nW m^{-2} sr^{-1})	Reference
1.25	42	<19		<200	Kashlinsky et al. 1996a
1.25	42	$15.5^{+3.7}_{-7.0}$			Kashlinsky et al. 2000[e]
1.25	42	<5.6			Wright 2001b
1.4	8	~18			Matsumoto et al. 2000
2.2	0.2–0.5	<9.6			Boughn et al. 1986[f]
2.2	1–5	<4.1			Boughn et al. 1986[f]
2.2	42	<7		<78	Kashlinsky et al. 1996a
2.2	42	$5.9^{+1.6}_{-3.7}$			Kashlinsky et al. 2000[e]
2.2	42	<2.5			Wright 2001b
2.6	8	~5			Matsumoto et al. 2000
3.5	42	<2.4		<26	Kashlinsky et al. 1996a
3.5	42	$2.4^{+0.5}_{-0.9}$			Kashlinsky et al. 2000[e]
4.9	42	<1.3		<13	Kashlinsky et al. 1996b
4.9	42	$2.0^{+0.25}_{-0.5}$			Kashlinsky et al. 2000[e]
12–100	42	≲1–1.5		≲10–15	Kashlinsky et al. 1996b
12	42	<1.0		<15	Kashlinsky et al. 2000
25	42	<0.5		<8	Kashlinsky et al. 2000
60	42	<0.8		<12	Kashlinsky et al. 2000
100	42	<1.1		<17	Kashlinsky et al. 2000
90	0.4–20		13000 ± 3000 (150 mJy)	>3–10	Matsuhara et al. 2000
170	0.6–4	~1	7400 (100 mJy)		Lagache & Puget 2000
170	0.6–20		12000 ± 2000 (250 mJy)	>0.9–2.6	Matsuhara et al. 2000
400–1000	420	$4(\lambda/400\ \mu\text{m})^{-3.1}$			Burigana & Popa 1998

[a]Approximate angular scale of fluctuation measurements.

[b]$[\delta(\nu I_\nu)]^2$ is the variance of νI_ν.

[c]Source power spectrum, for sources fainter than flux shown in parentheses.

[d]Reported limit on the CIB inferred from the fluctuation measurement.

[e]Limits give 92% confidence interval.

[f]90% confidence level.

Extragalactic Background Fluctuation

- Two-body correlation function of galaxies
  - Correlation function of galaxies brighter than the limiting magnitude
- Edxtra-galactic background fluctuation
  - Correlation function of galaxies dimmer than the limiting magnitude

Extragalactic Background Fluctuation

- Diffuse extra-galactic background light (EBL)
  - Superposition of unresolved galaxies ?(NIR)
- Expected outcome from EBL anisotropy
  - Source of EBL
  - Number of unresolved galaxies
- IR Satellite projects
  - SIRTF
  - Astro-F, SPICA

Extragalactic Background Fluctuation

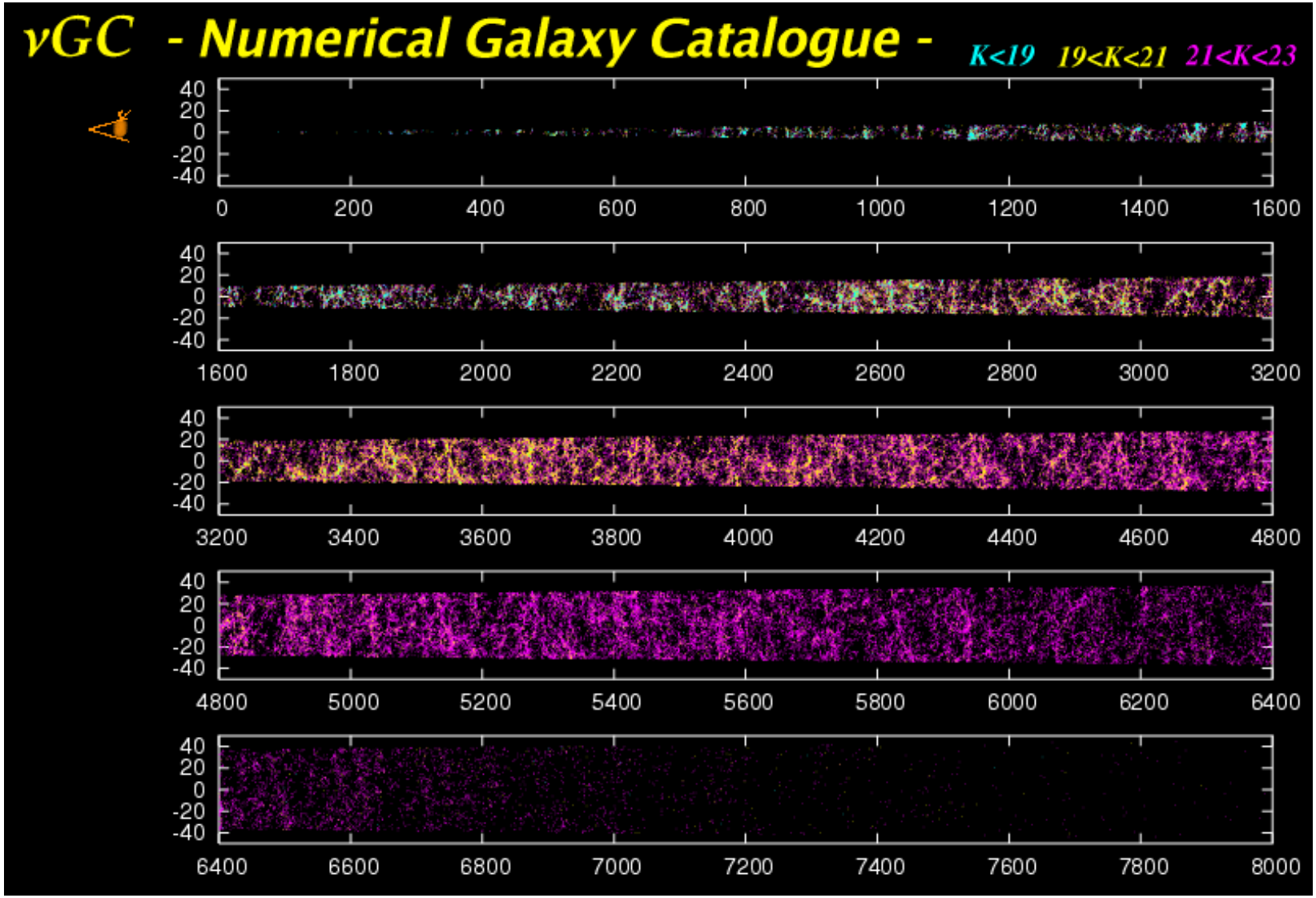

Extragalactic Background Fluctuation

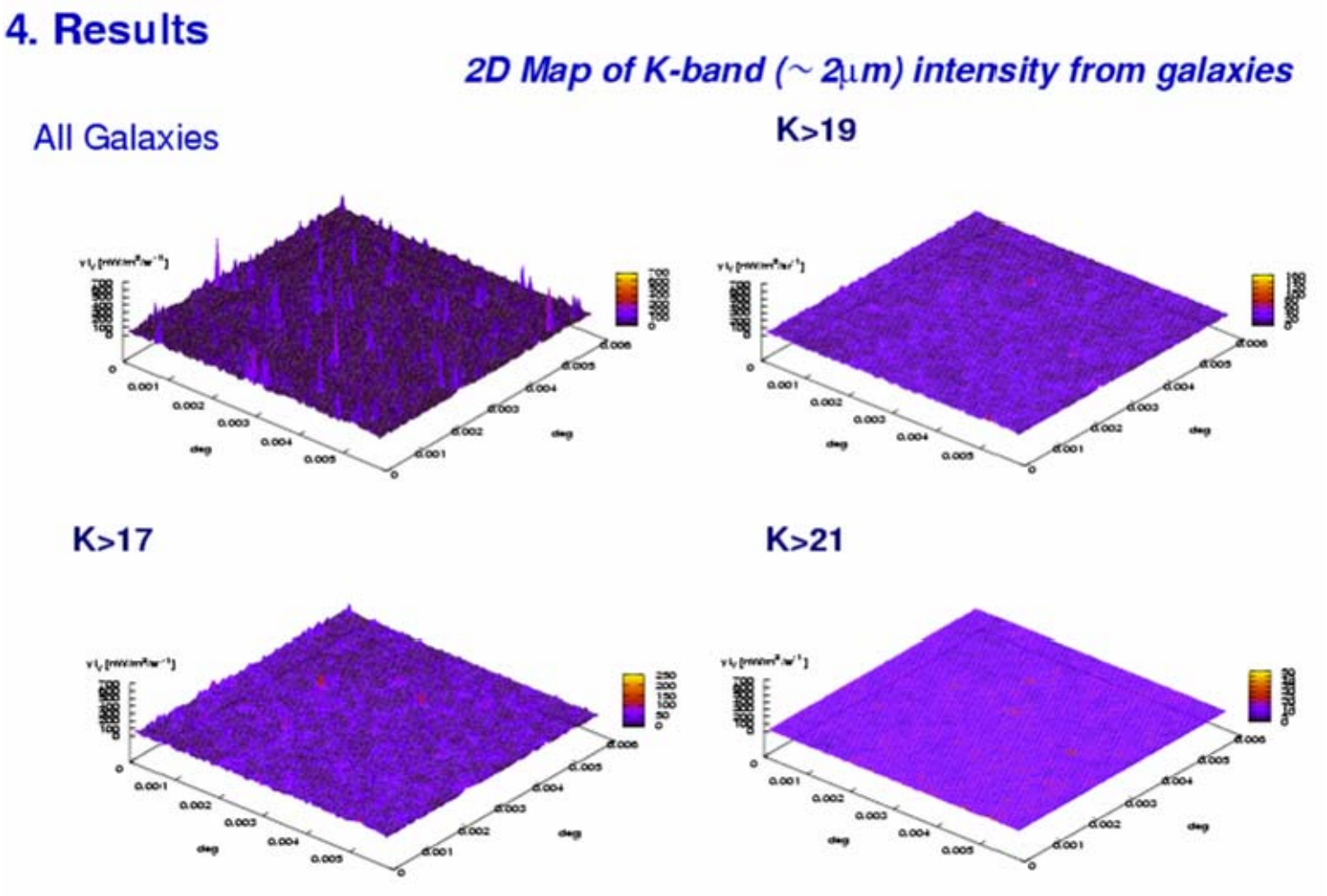

Extragalactic Background Fluctuation

- Kashlinsky et al. (2002)

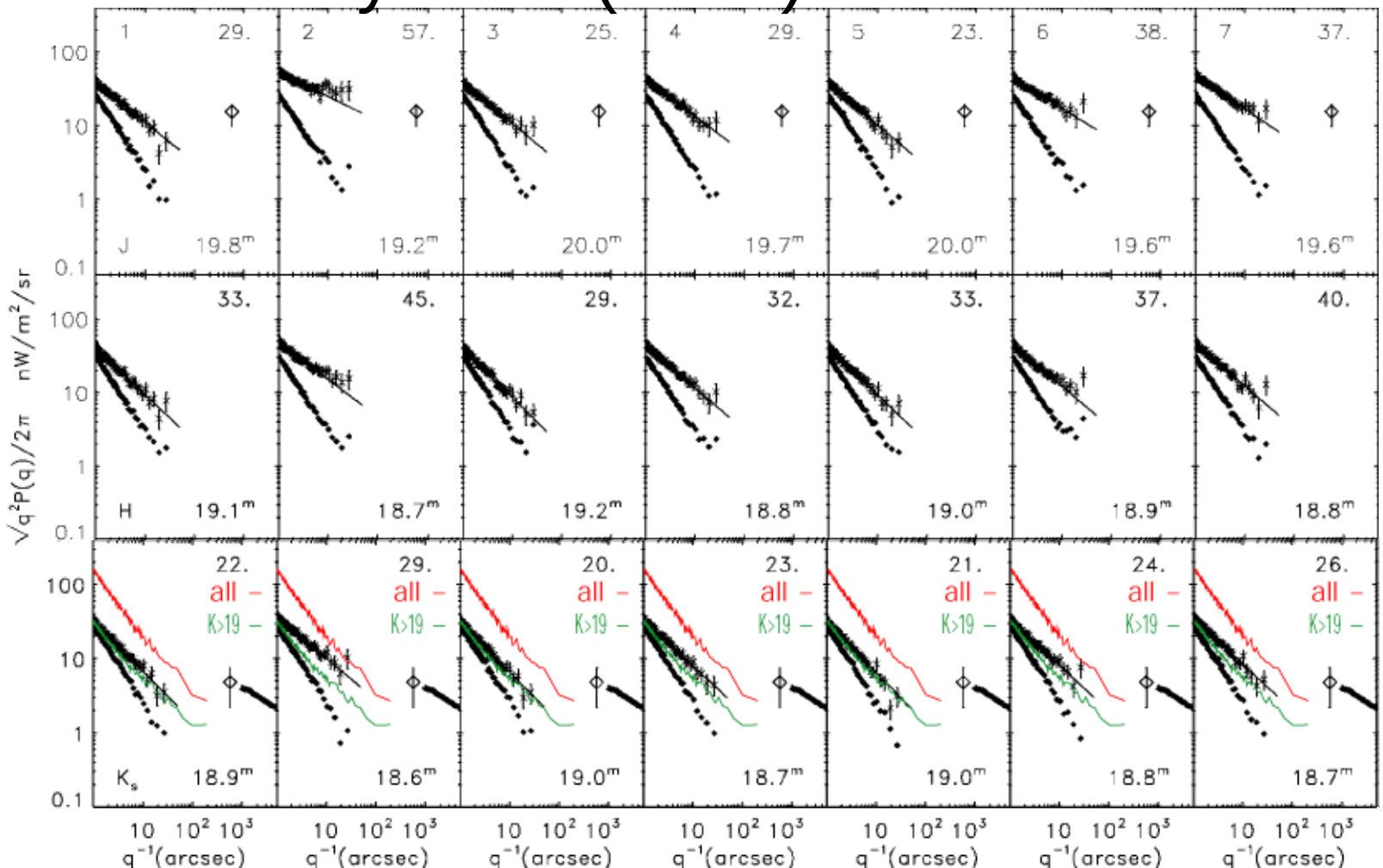

PISCES project

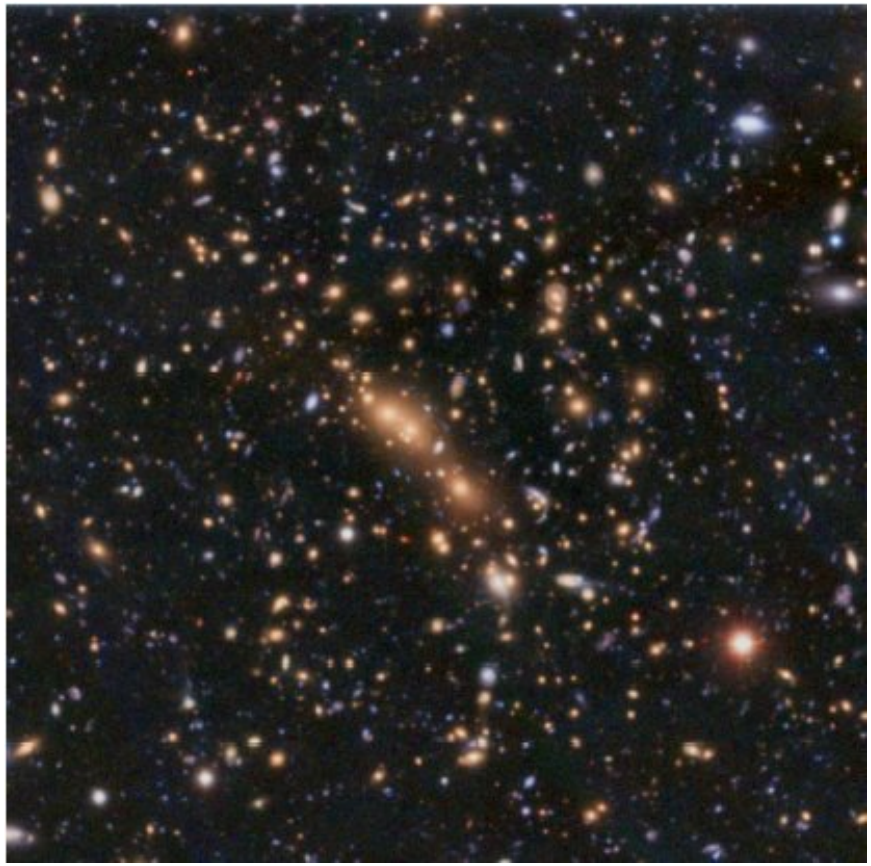

CL0016+1609

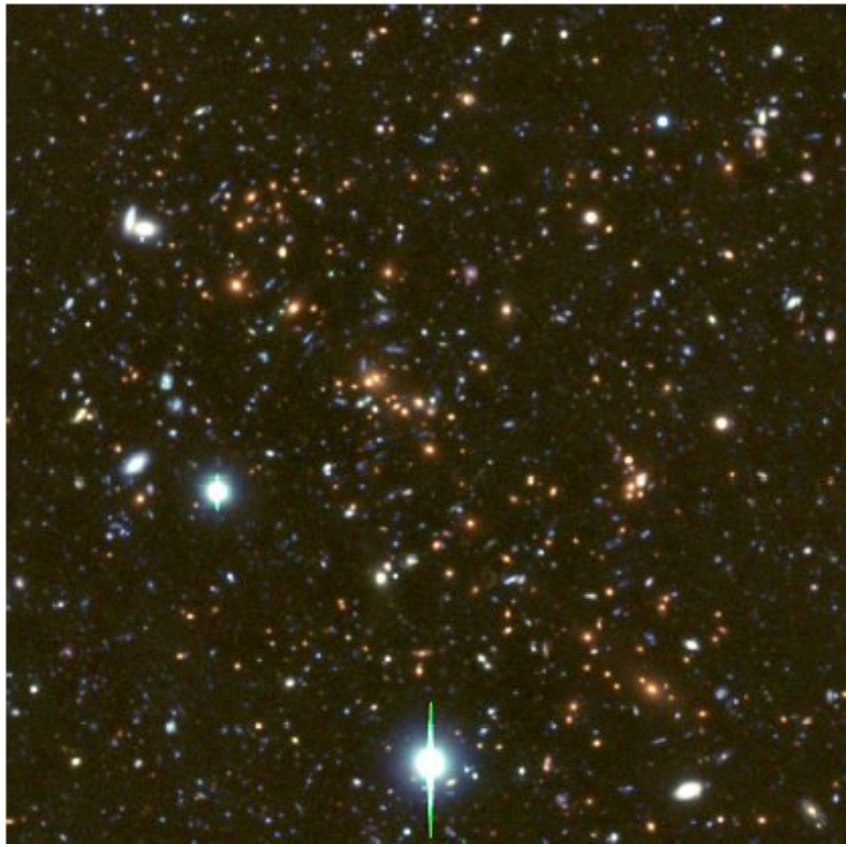

RX J0152.7-1357

- Suprime-CAM/Subaru

- 左:可視光の銀河分布
- 右:X線

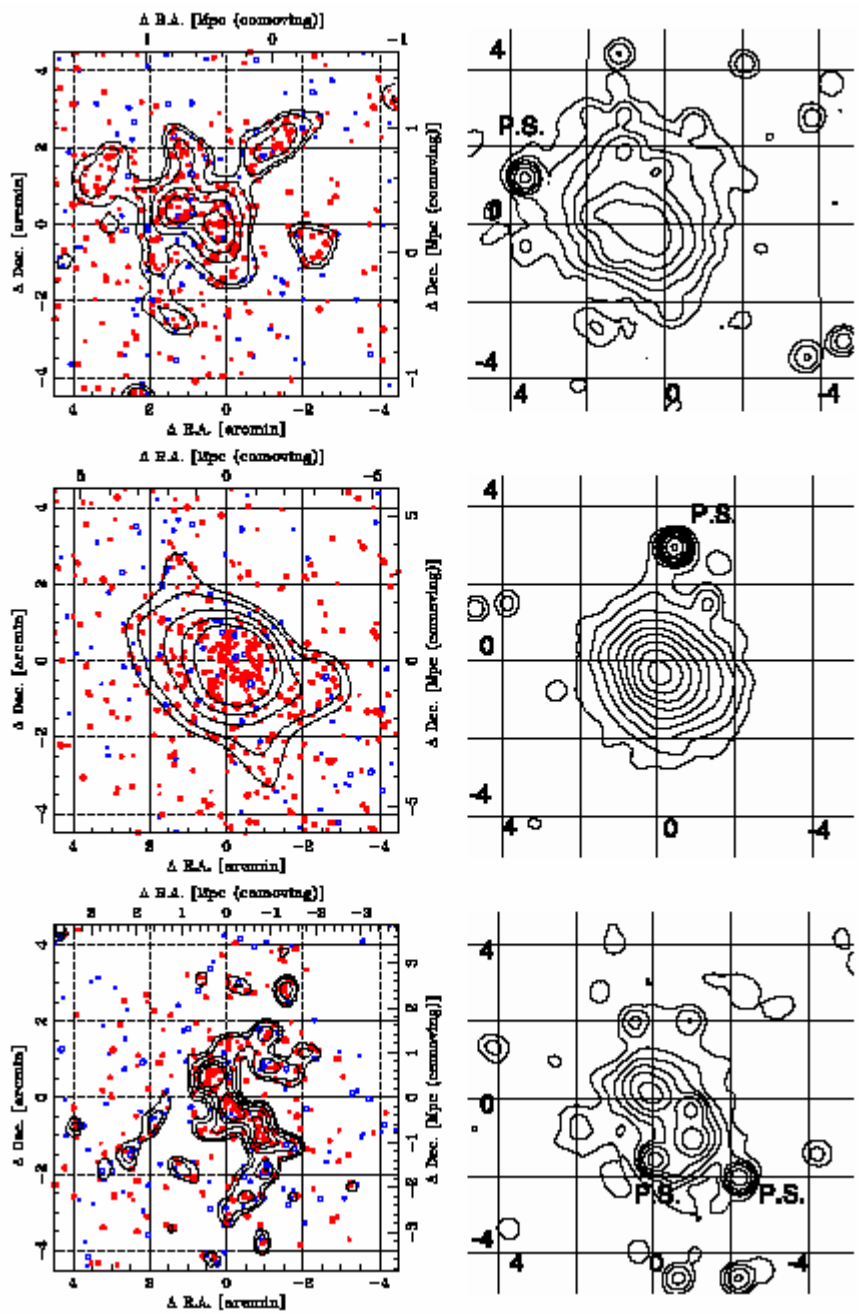

- 左:銀河団周辺の全銀河の分布
- 中央:赤い銀河の分布
- 右:同じ赤方偏移にあるνGC銀河団周辺の銀河分布

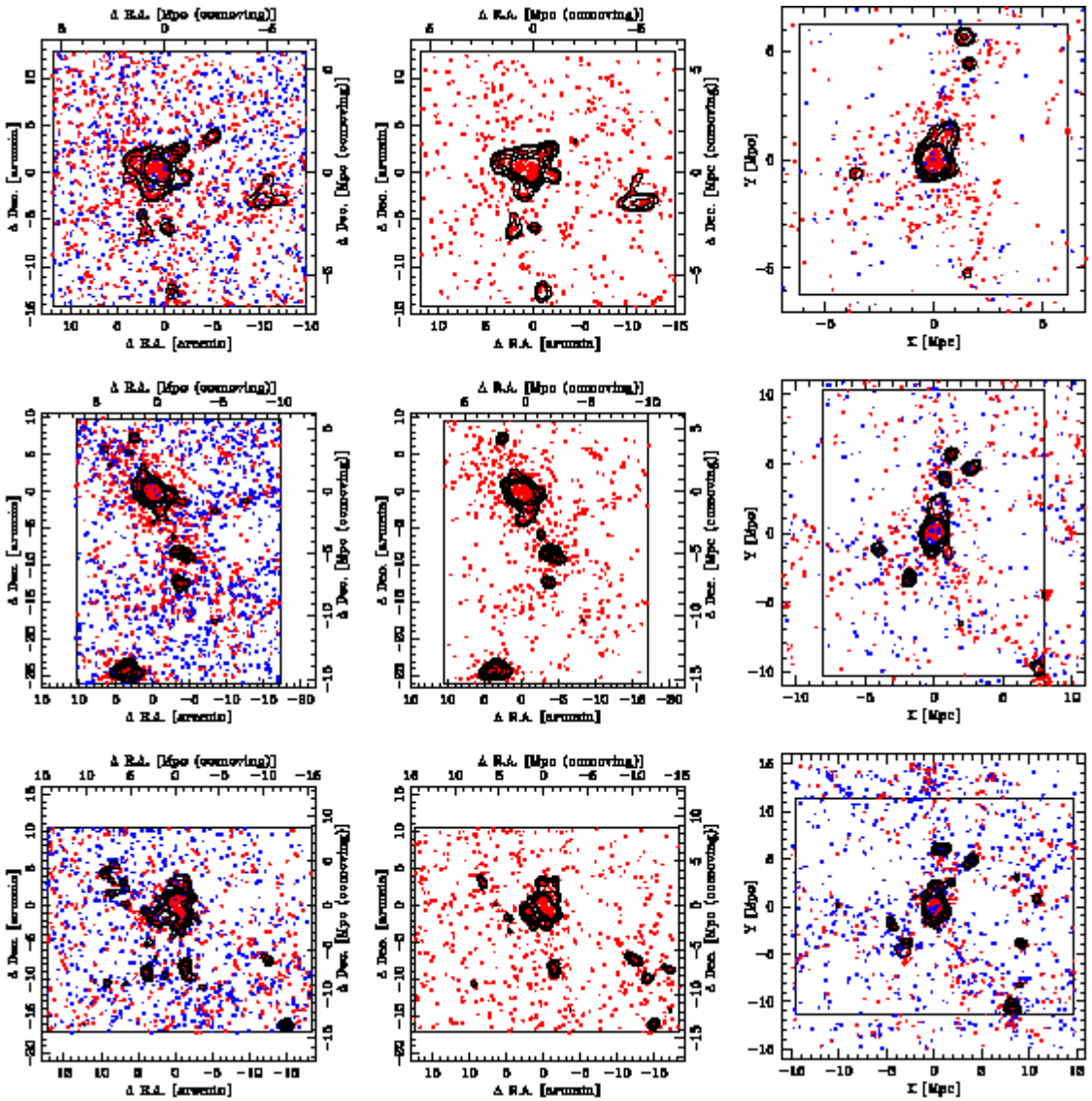

- $C=L^2/(4\pi S)$
- 左:実際の銀河団　右:νGC銀河団

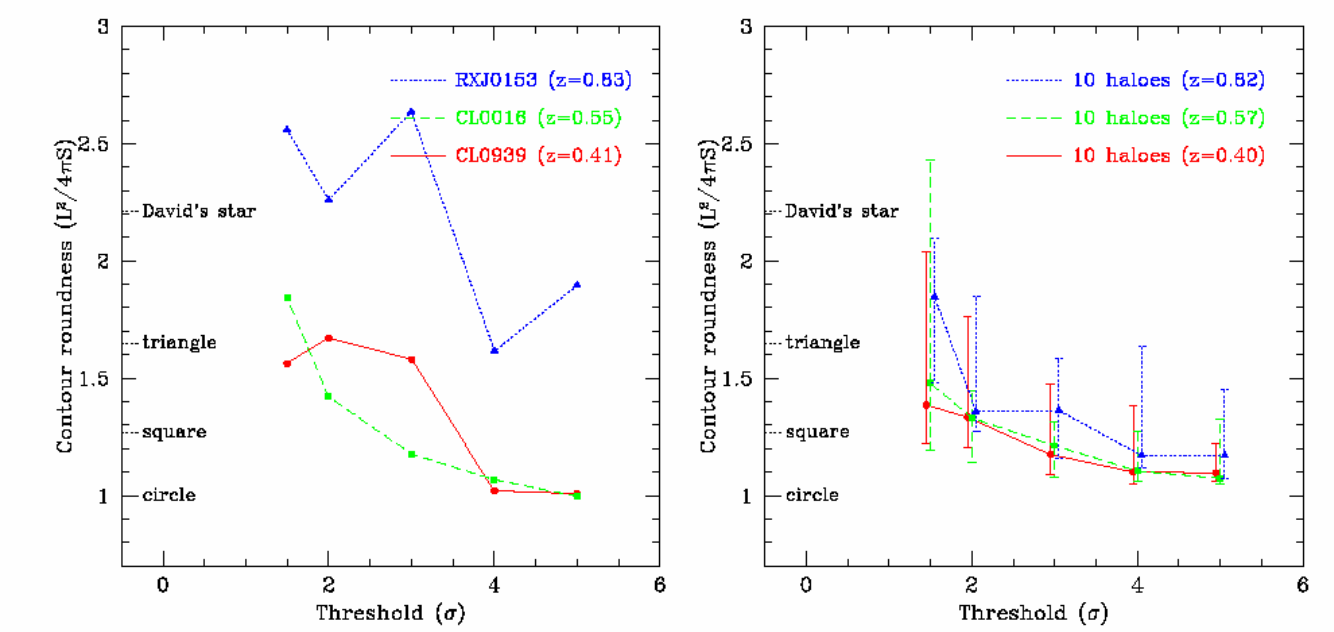

Fig. 6. Roundness of iso-density contours $L^2/(4\pi S)$ as a function of the threshold of the contours, where L is the length of the contour and S is the area surrounded by the contour. Only the major clump near or at the cluster center $(0, 0)$ is used. Observed data are plotted in the left panel, while the model predictions are shown in the right panel. The data points and the associated error-bars in the right panel show the median and 16%–84% range of the distribution of 10 model halos at each threshold, respectively.

- A=i/n- θ_i/360

$$P(\theta) = \left(\frac{1}{n}\sum_{i=1}^{n}\cos k\theta_i\right)^2 + \left(\frac{1}{n}\sum_{i=1}^{n}\sin k\theta_i\right)^2$$

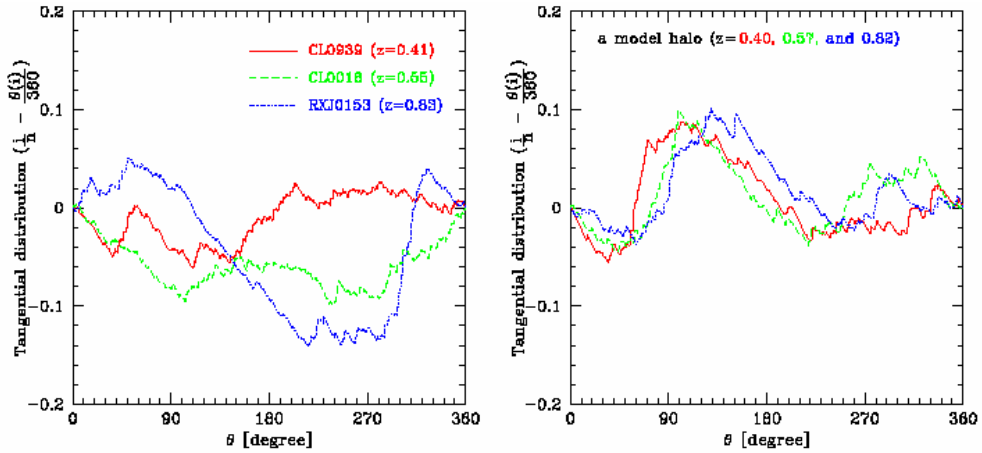

Fig. 8. Tangential galaxy distribution within the radial range of $0.3 < R_c < 1.5$ Mpc centerd on the positions of (ΔR.A., ΔDec.) = (0′.4, 0′.2), (0′, 0′), and (0′.4, 0′.6), for CL 0939, CL 0016, and RX J0153 clusters, respectively. The galaxies within the above radial range (total number is n) are sorted in order of θ, and the amplitude at the i-th galaxy at $\theta(i)$ is given by $i/n - \theta(i)/360°$. A straight line at zero would mean the uniform distribution of galaxies in the tangential direction (equal spacing in θ). The decrement and increment of the curves reflect the lower and higher densities compared to the averaged density, respectively (left panel). An example of our model cluster (most massive halo in our simulation) is shown in the right panel.

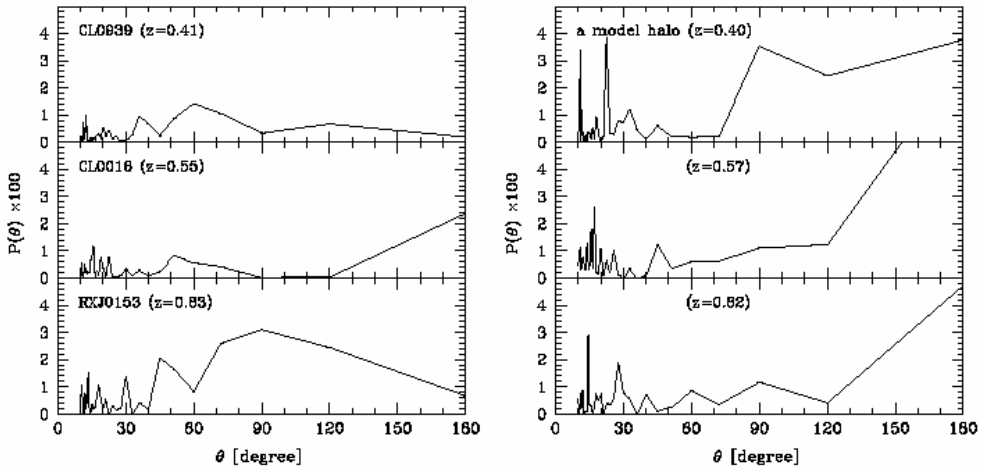

Fig. 9. Normalized power of the Fourier expansion of the galaxy distribution around the averaged density in the tangential direction, within the radial range of $0.3 < R_c < 1.5$ Mpc centerd on the positions of (ΔR.A., ΔDec.) = (0′.4, 0′.2), (0′, 0′), and (0′.4, 0′.6), for CL 0939, CL 0016, and RX J0153 clusters, respectively (left panel). An example of our model cluster (most massive halo in our simulation) is shown in the right panel.

LBG銀河の角度相関関数(ACF)

- SDFとνGCの比較

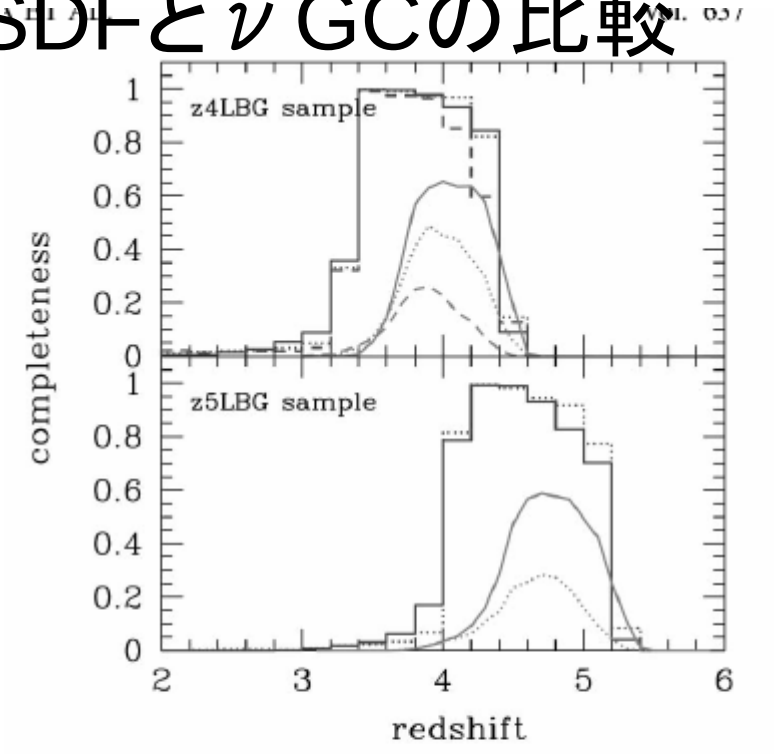

FIG. 1.—Sample completeness of the νGC mock LBG sample. The histograms show the completeness of the color-selected (COL-selected) νGC LBG sample, while the lines show the completeness estimate of the observed SDF LBG sample. *Top:* z4LBGs in $i' \leq 25.5$ (*solid line*), $25.5 < i' \leq 26.5$ (*dotted line*), and $25.5 < i' \leq 27.4$ (*dashed line*). *Bottom:* z5LBGs in $z' \leq 25.75$ (*solid line*) and $25.75 < z' \leq 26.6$ (*dotted line*). The completeness of the SDF LBG sample by Yoshida et al. (2005) was rebinned in magnitudes from the original plot taking the average with number weighting. [*See the electronic edition of the Journal for a color version of this figure.*]

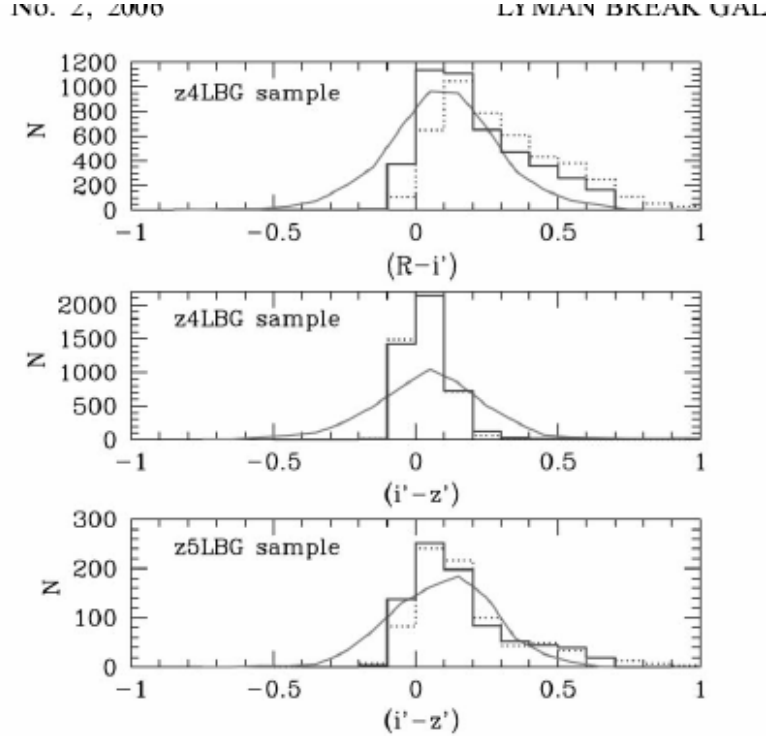

FIG. 2.—Comparison of the rest-UV color distribution for LBGs at $z \sim 4$ (*top and middle*) and $z \sim 5$ (*bottom*) between SDF observations (*solid lines*) and the predictions of the νGC (*histograms*). The solid histograms denote the color distribution of COL-selected νGC LBG samples, while the dotted histograms are those of SF-selected νGC LBG samples. [*See the electronic edition of the Journal for a color version of this figure.*]

光度関数の比較

- COLサンプル(実線)
  - SDFデータと同じ条件で選別
- SFサンプル(点線)
  - SDF銀河の赤方偏移と等級が一致するように乱数を振って選別

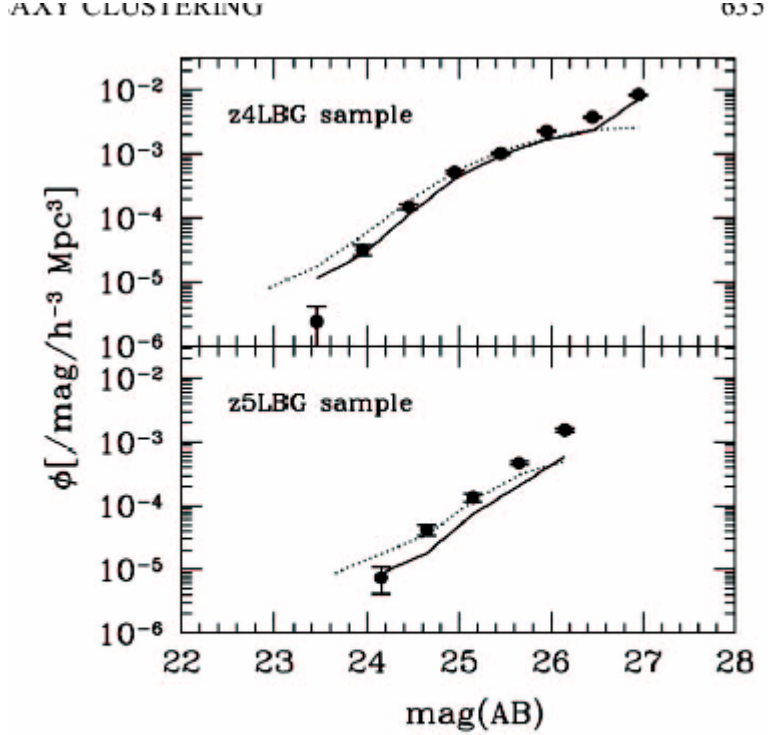

FIG. 3.—Comparison of the luminosity functions for LBGs at $z \sim 4$ (*top*) and $z \sim 5$ (*bottom*) between SDF observations by Yoshida et al. (2005; *circles with error bars*) and the predictions of the νGC (*lines*). The solid lines denote the luminosity functions of COL-selected νGC LBG samples, while the dotted lines are those of SF-selected νGC LBG samples. [*See the electronic edition of the Journal for a color version of this figure.*]

空間分布

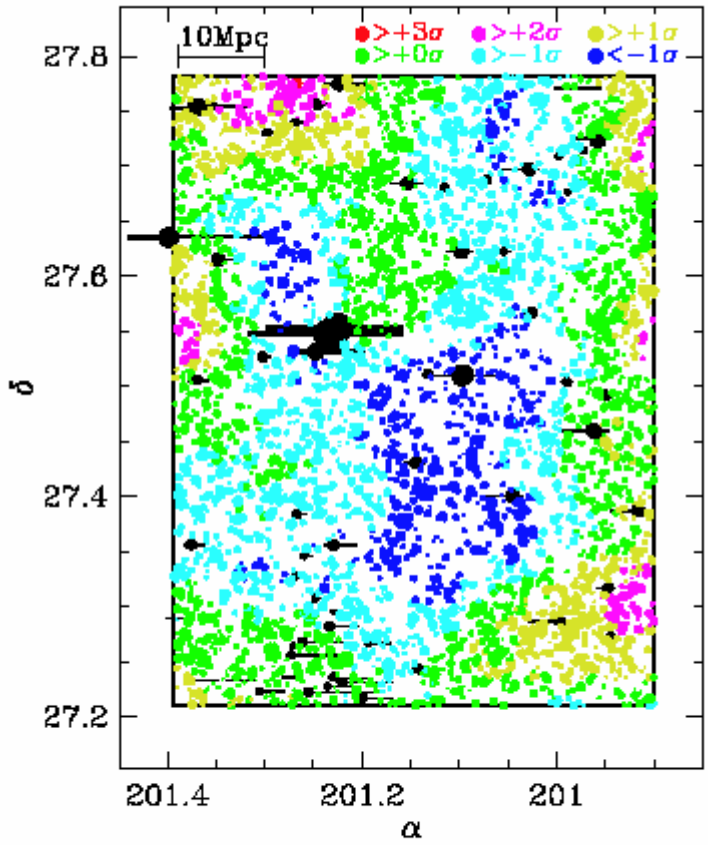

FIG. 4.—Sky distribution of SDF z4LBG sample. Larger circles denote brighter objects in total i'-band magnitude. The local overdensity, with the significance of each, is denoted by color as shown in the color legend. The black shaded areas are masked regions in which detected objects were rejected due to low S/N. North is up and east is to the left.

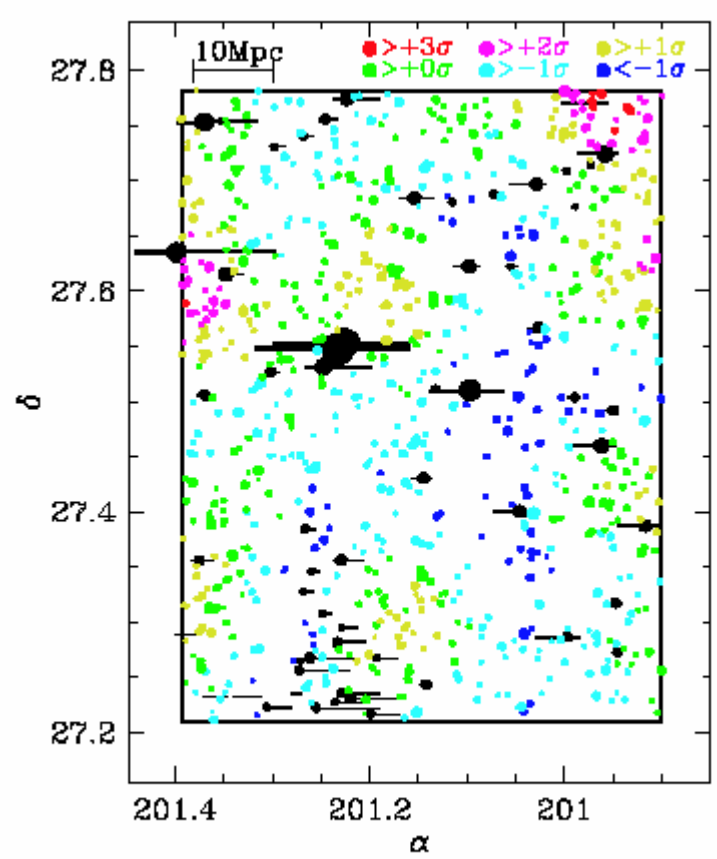

FIG. 5.—Same sky distribution as in Fig. 4, but for the SDF z5LBG sample.

ACF

- 実線:IC入り冪関数フィット
- 点線:Ouchi et al. (2004)

TABLE 1
ACF Parameters of SDF LBG Samples

Sample	N[a]	f_c[b] (%)	β[c]	A_w[c]	r_0[d]
z4LBG total	4543	2.6	$-0.90^{+0.06}_{-0.04}$	$2.31^{+0.44}_{-0.45}$	$4.69^{+0.81}_{-0.67}$
z4LBG $i' \leq 25.5$	916	0.38	$-1.25^{+0.19}_{-0.25}$	$10.44^{+6.99}_{-4.36}$	$6.52^{+4.09}_{-2.50}$
z4LBG $25.5 < i' \leq 26.5$	1977	2.3	$-0.98^{+0.10}_{-0.12}$	$3.59^{+1.58}_{-1.14}$	$5.38^{+1.97}_{-1.44}$
z4LBG $26.5 < i' \leq 27.43$	1650	5.1	$-0.80^{+0.18}_{-0.16}$	$1.48^{+1.07}_{-0.76}$	$4.09^{+2.77}_{-1.66}$
z4LBG $(i'-z') > 0.0$	1124	...	$-1.08^{+0.12}_{-0.10}$	$5.94^{+2.00}_{-1.96}$	$6.14^{+2.12}_{-1.58}$
z4LBG $(i'-z') \leq 0.0$	653	...	$-1.04^{+0.50}_{-0.66}$	$2.47^{+7.08}_{-2.15}$	$4.19^{+13.7}_{-3.05}$
z5LBG total	831	10	$-1.02^{+0.14}_{-0.16}$	$7.16^{+2.92}_{-2.33}$	$6.09^{+2.66}_{-1.88}$
z5LBG $z' \leq 25.75$	325	9.0	$-1.15^{+0.15}_{-0.19}$	$18.68^{+7.43}_{-5.92}$	$8.16^{+3.76}_{-2.57}$
z5LBG $25.75 < z' \leq 26.62$	506	11	$-0.85^{+0.27}_{-0.26}$	$3.03^{+2.85}_{-1.77}$	$4.78^{+5.24}_{-2.38}$

[a] Number of sources in the sample.
[b] Contamination rate rebinned in magnitudes from the original estimate by Yoshida et al. (2005) taking the average with number weighting.
[c] The ACF power-law fitting parameters defined in eq. (4) with contamination correction.
[d] The correlation length inferred from ACF.

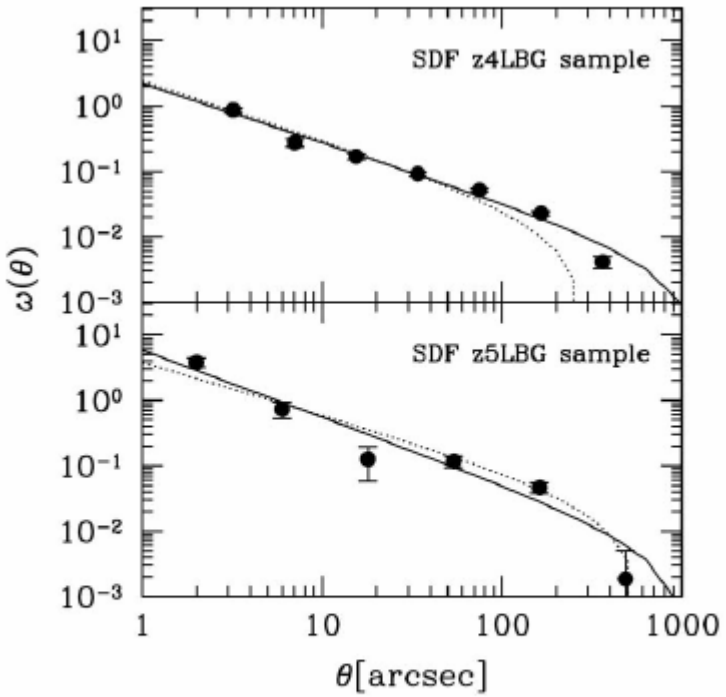

FIG. 6.—ACFs of z4LBG (*top*) and z5LBG (*bottom*) samples. The solid lines show the power-law fits with IC corrections. Error bars show the 1 σ Poissonian errors. The dotted lines show the ACF power law of the previous estimates in SDF by Ouchi et al. (2004b). [*See the electronic edition of the Journal for a color version of this figure.*]

ACFの光度依存性

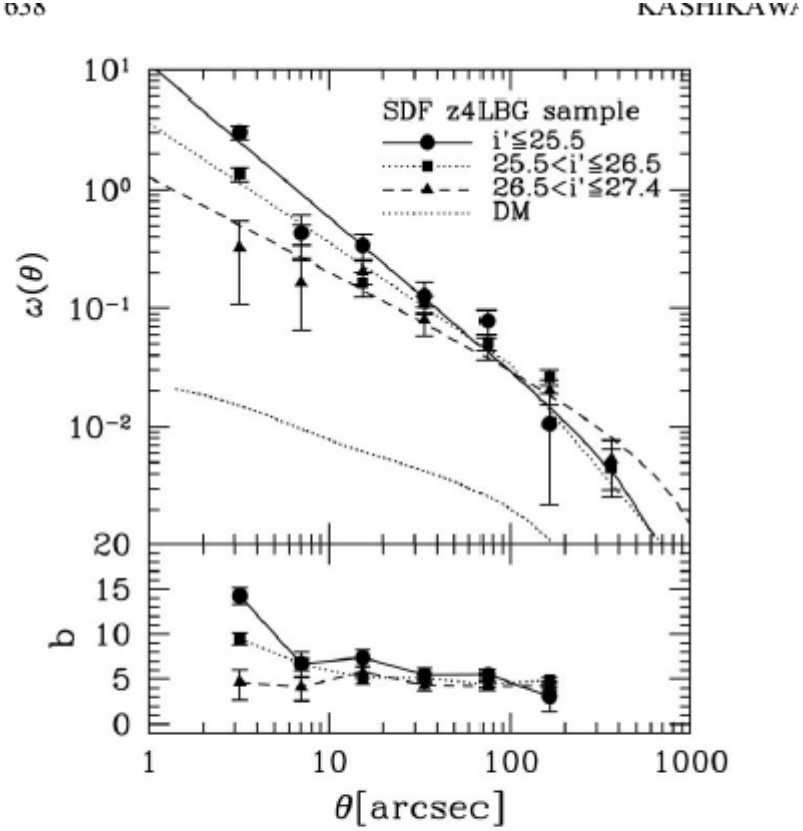

FIG. 7.—Luminosity dependence of ACFs in the z4LBG sample. The ACFs of $i' \leq 25.5$, $25.5 < i' \leq 26.5$, and $26.5 < i' \leq 27.4$ are represented by symbols given in the legend. The dotted line is the nonlinear ACF of dark matter at $z = 4$ calculated with the same observational selection function. *Bottom:* Our defined bias parameter $b(\theta)$ for each luminosity subsample with the same symbol as indicated in the top panel. [*See the electronic edition of the Journal for a color version of this figure.*]

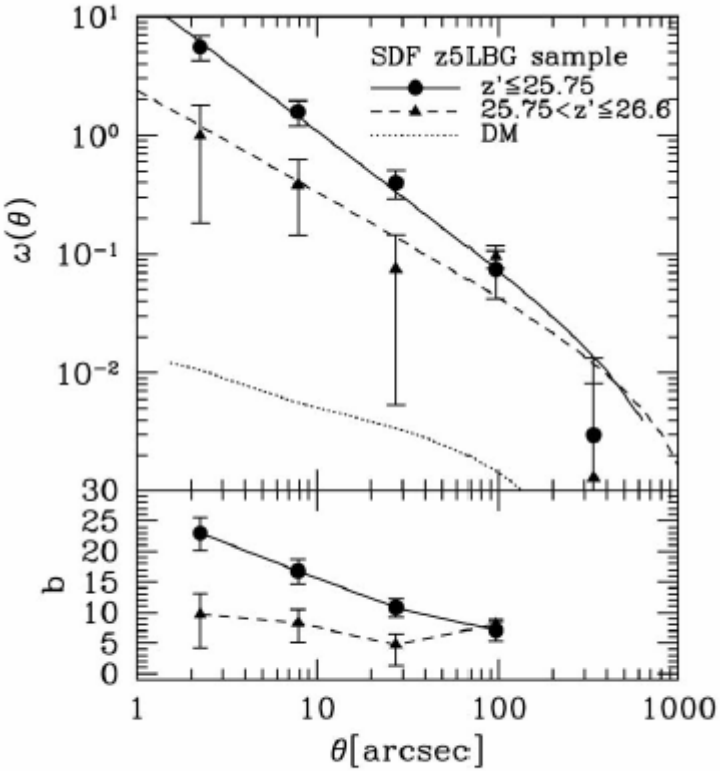

FIG. 8.—Same as Fig. 7, but for the SDF z5LBG sample. The ACFs of $z' \leq 25.75$ and $25.75 < z' \leq 26.6$ are represented by symbols given in the legend. [*See the electronic edition of the Journal for a color version of this figure.*]

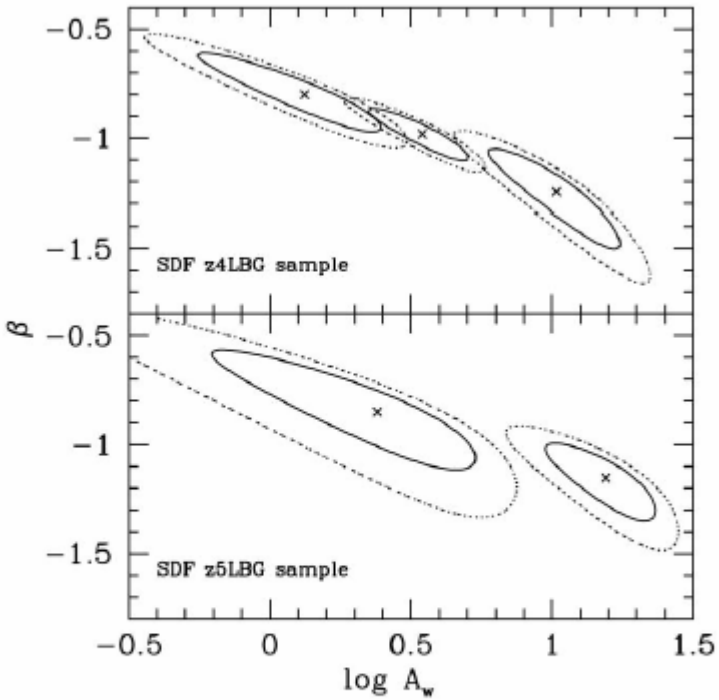

FIG. 9.—Error ellipses of derived ACF parameters of A_w and β for luminosity subsamples of z4LBGs (*top*) and z5LBGs (*bottom*). Ellipses from left to right denote from fainter to brighter luminosity subsamples. The solid and dotted ellipses are the 1 and 3 σ confidence levels. [*See the electronic edition of the Journal for a color version of this figure.*]

νGCのACF

- ●COL、○SF　　COL-ACFの光度依存性

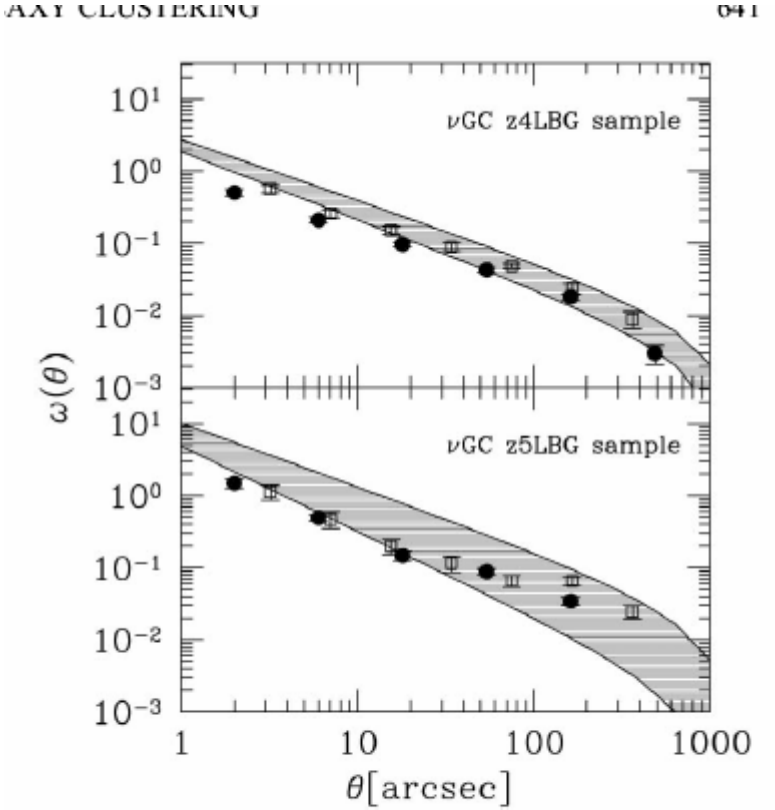

FIG. 12.—Model-predicted ACFs by νGC mock samples for z4LBGs (*top*) and z5LBGs (*bottom*). The filled circles and open squares denote the COL-selected and SF-selected samples, respectively. The shaded regions show the observed ACF of the SDF total sample with 1 σ tolerance. [*See the electronic edition of the Journal for a color version of this figure.*]

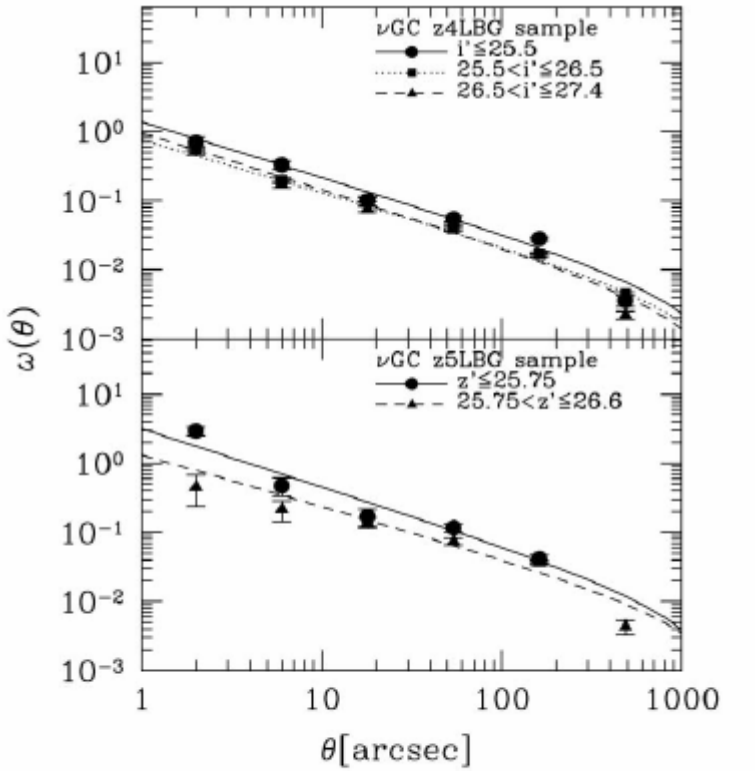

FIG. 13.—Luminosity dependence of ACFs in the νGC prediction of the COL-selected sample for z4LBGs (*top*) and z5LBGs (*bottom*). The symbols are identical to those in Figs. 7 and 8. [*See the electronic edition of the Journal for a color version of this figure.*]

TABLE 2
ACF Parameters of νGC LBG Samples

Sample	N^a	$f_c{}^a$ (%)	β	A_w
z4LBG total COL-selected	12712	5.6	$-0.74^{+0.04}_{-0.06}$	$0.83^{+0.22}_{-0.11}$
z4LBG total SF-selected	6653	0.0	-0.74 ± 0.08	$1.26^{+0.33}_{-0.35}$
z4LBG $i' \leq 25.5$	4979	4.6	$-0.80^{+0.06}_{-0.04}$	$1.38^{+0.28}_{-0.33}$
z4LBG $25.5 < i' \leq 26.5$	10735	6.4	$-0.76^{+0.02}_{-0.04}$	$0.76^{+0.11}_{-0.10}$
z4LBG $26.5 < i' \leq 27.4$	11742	6.0	$-0.82^{+0.04}_{-0.02}$	$0.95^{+0.10}_{-0.16}$
z4LBG $12.0 < \log(M_h/M_\odot)$	2928	0.0	-1.39 ± 0.01	44.19 ± 0.49
z4LBG $11.7 < \log(M_h/M_\odot) \leq 12.0$	4556	0.0	$-1.32^{+0.06}_{-0.26}$	$13.32^{+5.74}_{-1.14}$
z4LBG $11.5 < \log(M_h/M_\odot) \leq 11.7$	5174	0.0	$-0.92^{+0.08}_{-0.04}$	$2.01^{+0.39}_{-0.50}$
z4LBG $11.3 < \log(M_h/M_\odot) \leq 11.5$	7201	0.0	$-0.77^{+0.11}_{-0.03}$	$0.69^{+0.14}_{-0.26}$
z4LBG $\log(M_h/M_\odot) \leq 11.3$	5983	0.0	$-0.64^{+0.14}_{-0.11}$	$0.37^{+0.21}_{-0.16}$
z4LBG 1halo-1LBG $12.0 < \log(M_h/M_\odot)$	1796	0.0	-0.82 ± 0.12	$2.88^{+2.13}_{-1.22}$
z4LBG 1halo-1LBG $11.7 < \log(M_h/M_\odot) \leq 12.0$	3783	0.0	-0.88 ± 0.12	$2.00^{+1.47}_{-0.85}$
z4LBG 1halo-1LBG $11.5 < \log(M_h/M_\odot) \leq 11.7$	4931	0.0	$-0.80^{+0.12}_{-0.10}$	$0.96^{+0.56}_{-0.45}$
z4LBG 1halo-1LBG $11.3 < \log(M_h/M_\odot) \leq 11.5$	7135	0.0	-0.86 ± 0.10	$0.87^{+0.51}_{-0.32}$
z4LBG 1halo-1LBG $\log(M_h/M_\odot) \leq 11.3$	5960	0.0	$-0.85^{+0.19}_{-0.16}$	$0.67^{+0.59}_{-0.37}$
z5LBG total COL-selected	2603	0.5	$-0.81^{+0.09}_{-0.07}$	$2.06^{+0.45}_{-0.48}$
z5LBG total SF-selected	1690	0.0	$-0.86^{+0.18}_{-0.22}$	$2.56^{+1.80}_{-1.25}$
z5LBG $z' \leq 25.75$	1611	0.12	$-0.84^{+0.12}_{-0.10}$	$3.17^{+1.40}_{-1.20}$
z5LBG $25.75 < z' \leq 26.6$	3101	1.2	-0.74 ± 0.06	$1.32^{+0.42}_{-0.36}$
z5LBG $12.1 < \log(M_h/M_\odot)$	440	0.0	$-1.24^{+0.08}_{-0.06}$	$49.70^{+7.85}_{-8.01}$
z5LBG $11.8 < \log(M_h/M_\odot) \leq 12.1$	1117	0.0	-1.04 ± 0.06	$13.40^{+1.73}_{-2.44}$
z5LBG $11.5 < \log(M_h/M_\odot) \leq 11.8$	2547	0.0	-0.90 ± 0.08	$2.40^{+0.91}_{-0.74}$
z5LBG 1halo-1LBG $12.1 < \log(M_h/M_\odot)$	385	0.0	$-0.84^{+0.30}_{-0.28}$	$7.59^{+14.3}_{-5.77}$
z5LBG 1halo-1LBG $11.8 < \log(M_h/M_\odot) \leq 12.1$	1029	0.0	$-0.64^{+0.18}_{-0.14}$	$2.09^{+1.89}_{-1.18}$
z5LBG 1halo-1LBG $11.5 < \log(M_h/M_\odot) \leq 11.8$	2486	0.0	$-0.72^{+0.18}_{-0.10}$	$1.33^{+0.86}_{-0.72}$

[a] N and f_c are average values for the random resampling process for the total and luminosity subsamples.

ν GC-ACFの質量依存性

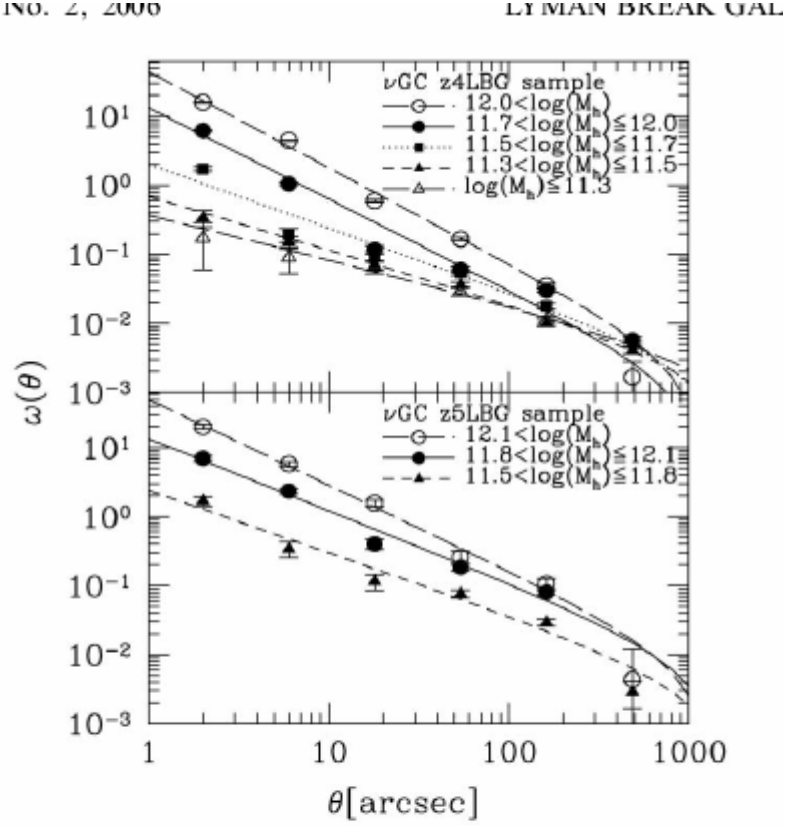

FIG. 14.—Halo mass dependence of ACFs in νGC for z4LBGs (*top*) and z5LBGs (*bottom*). The halo mass subsamples of $12.0 < \log(M_h/M_\odot)$, $11.7 < \log(M_h/M_\odot) \leq 12.0$, $11.5 < \log(M_h/M_\odot) \leq 11.7$, $11.3 < \log(M_h/M_\odot) \leq 11.5$, and $\log(M_h/M_\odot) \leq 11.3$ are represented by symbols as shown in the legend, from top to bottom for z4LBGs. The mass subsamples of $12.1 < \log(M_h/M_\odot)$, $11.8 < \log(M_h/M_\odot) \leq 12.1$, and $11.5 < \log(M_h/M_\odot) \leq 11.8$ are are represented by symbols as shown in the legend, from top to bottom for z5LBGs. [*See the electronic edition of the Journal for a color version of this figure.*]

Multiplicity

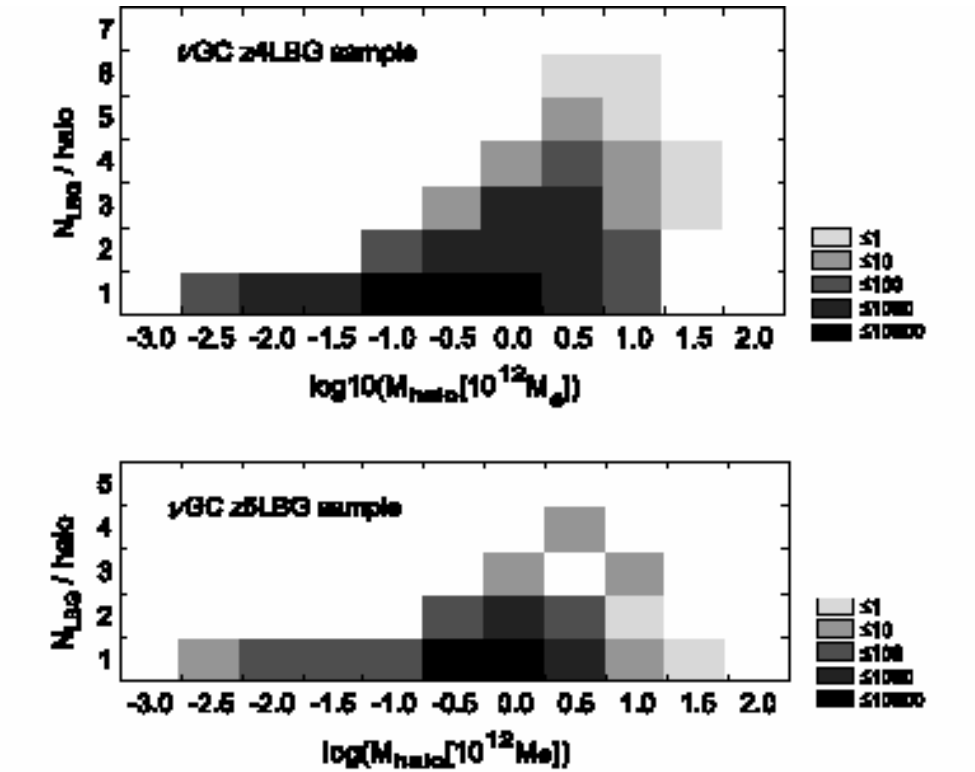

FIG. 15.—Two-dimensional histograms of the dark halo mass and the LBG occupation number in a halo predicted by the νGC for z4LBGs (*top*) and z5LBGs (*bottom*). Each color level shows the number of galaxies as shown in the gray-scale legend; the darker shaded region shows greater numbers of samples. The halo mass $M_{\rm halo}$ is shown in units of 10^{12} $M_{\odot}$. [*See the electronic edition of the Journal for a color version of this figure.*]

冪関数フィットの質量依存性

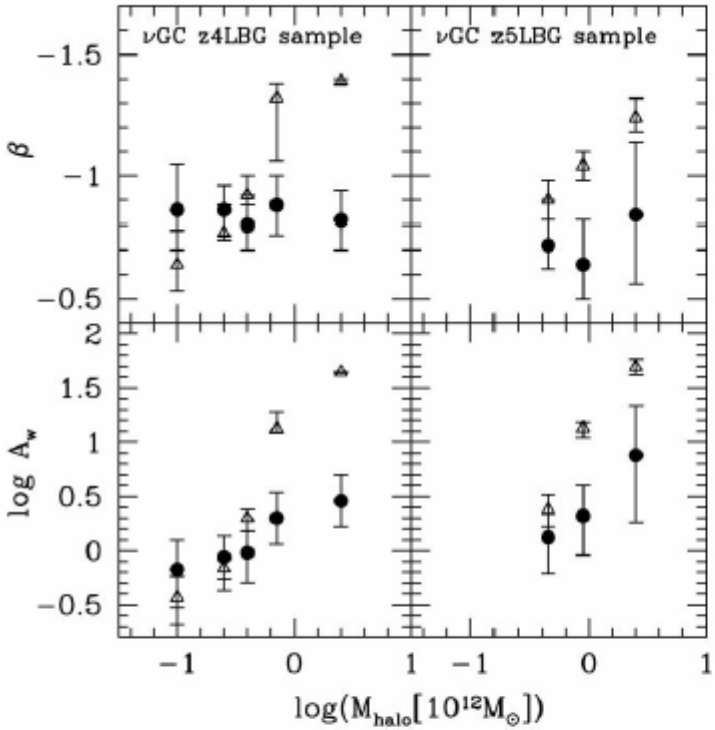

FIG. 16.—ACF parameters, β and A_w, of the halo-mass–distinct subsamples in the νGC 1halo-1LBG catalog. The circles denote the ACF parameters of the 1halo-1LBG sample, while the triangles denote those of the original mock catalog derived in Fig. 14 for comparison. *Left:* ACF slope β (*top*) and ACF amplitude A_w (*bottom*) of the z4LBG sample as a function of dark halo mass. *Right:* Same as left, but for the z5LBG sample. [*See the electronic edition of the Journal for a color version of this figure.*]

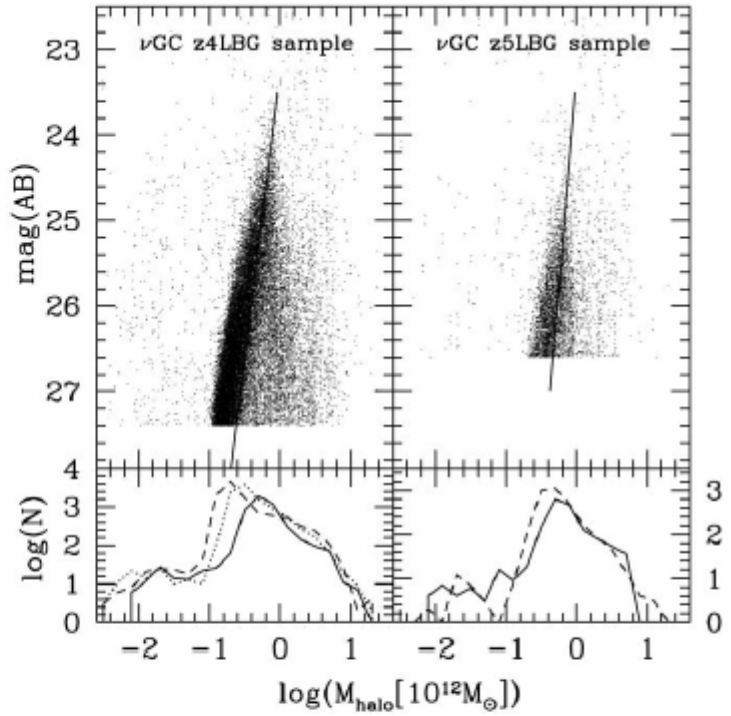

FIG. 17.—Prediction of νGC regarding the UV luminosity–dependence of galactic halo mass. The magnitudes quoted are for the i' band in the z4LBG sample (*top left*) and the z' band in the z5LBG sample (*top right*). The straight lines show the linear fit to the mean ridge of the distribution. *Bottom:* Halo mass histograms for each luminosity subsample with the same lines as indicated in Figs. 7 and 8. [*See the electronic edition of the Journal for a color version of this figure.*]

Summary

- N-body + SAM = ν GC
  - High mass resolution
    - Parallelized AMR N-body simulation code
- Comparison with observation
  - Angular correlation function
    - Our catalog realizes the observational data
  - Extragalactic background light
    - Our catalog fits the 2MASS results quite well
    - What is the origin of the excess at 10mins< ?